Brain, Behavior, and Immunity xxx (xxxx) xxx

Contents lists available at ScienceDirect

Brain Behavior and Immunity

journal homepage: www.elsevier.com/locate/ybrbi

Full-length Article

Kefir ameliorates specific microbiota-gut-brain axis impairments in a mouse model relevant to autism spectrum disorder

Marcel van de Wouw [a,b,1], Calum J. Walsh [a,e,1], Giulia M.D. Vigano [a,c], Joshua M. Lyte [a], Marcus Boehme [a], Andreu Gual-Grau [a,d], Fiona Crispie [a,e], Aaron M. Walsh [a,e,f], Gerard Clarke [a,g], Timothy G. Dinan [a,g], Paul D. Cotter [a,e,*,2], John F. Cryan [a,b,g,*,2]

[a] APC Microbiome Ireland, University College Cork, Cork, Ireland
[b] Department of Anatomy and Neuroscience, University College Cork, Cork, Ireland
[c] Department of Pharmacological and Biomolecular Sciences, University of Milan, Italy
[d] Nutrigenomics Research Group, Biochemistry and Biotechnology Department, Rovira i Virgili University, Tarragona, Spain
[e] Teagasc Food Research Centre, Moorepark, Fermoy, Cork, Ireland
[f] School of Microbiology, University College Cork, Cork, Ireland
[g] Department of Psychiatry and Neurobehavioural Science, University College Cork, Cork, Ireland

ARTICLE INFO

Keywords:
Kefir
Microbiome
Stress
Immunity
Behaviour
Autism spectrum disorder

ABSTRACT

Autism spectrum disorder (ASD) is one of the most severe developmental disorders, affecting on average 1 in 150 children worldwide. There is a great need for more effective strategies to improve quality of life in ASD subjects. The gut microbiome has emerged as a potential therapeutic target in ASD. A novel modulator of the gut microbiome, the traditionally fermented milk drink kefir, has recently been shown to modulate the microbiota and decrease repetitive behaviour, one of the hallmarks of ASD, in mice. As such, we hypothesized that kefir could ameliorate behavioural deficits in a mouse model relevant to ASD; the BTBR T^{+} $Itpr3^{tf}$/J mouse strain. To this end, adult mice were administered either kefir (UK4) or a milk control for three weeks as treatment lead-in, after which they were assessed for their behavioural phenotype using a battery of tests. In addition, we assessed systemic immunity by flow cytometry and the gut microbiome using shotgun metagenomic sequencing. We found that indeed kefir decreased repetitive behaviour in this mouse model. Furthermore, kefir prolonged stress-induced increases in corticosterone 60 min post-stress, which was accompanied by an ameliorated innate immune response as measured by $LY6C^{hi}$ monocyte levels. In addition, kefir increased the levels of anti-inflammatory Treg cells in mesenteric lymph nodes (MLNs). Kefir also increased the relative abundance of *Lachnospiraceae bacterium A2*, which correlated with reduced repetitive behaviour and increased Treg cells in MLNs. Functionally, kefir modulated various predicted gut microbial pathways, including the gut-brain module S-Adenosylmethionine (SAM) synthesis, as well as L-valine biosynthesis and pyruvate fermentation to isobutanol, which all correlated with repetitive behaviour. Taken together our data show that kefir modulates peripheral immunoregulation, can ameliorate specific ASD behavioural dysfunctions and modulates selective aspects of the composition and function of the gut microbiome, indicating that kefir supplementation might prove a viable strategy in improving quality of life in ASD subjects.

Abbreviations: ASD, autism spectrum disorder; Treg, T regulatory cell; MLN, Mesenteric lymph node; pTreg, Peripheral-derived T regulatory cells; 5-HT, Serotonin; 5-HIAA, 5-hydroxyindoleacetic acid; LeFse, Linear discriminant analysis Effect Size.

* Corresponding authors at: APC Microbiome Ireland, Department of Anatomy and Neuroscience, University College Cork, Cork, Ireland (J.F. Cryan). APC Microbiome Ireland, Teagasc Food Research Centre, Moorepark, Fermoy, Co. Cork, Ireland (P.D. Cotter).
E-mail addresses: paul.cotter@teagasc.ie (P.D. Cotter), j.cryan@ucc.ie (J.F. Cryan).
[1] Shared first co-author.
[2] Shared last co-author.

https://doi.org/10.1016/j.bbi.2021.07.004
Received 16 May 2021; Received in revised form 17 June 2021; Accepted 3 July 2021
Available online 9 July 2021

1. Introduction

Autism spectrum disorder (ASD) is one of the most severe and pervasive neurodevelopmental conditions, affecting on average 1 in 150 children worldwide (Lyall et al., 2017). ASD is hallmarked by impaired social communication skills and enhanced engagement in repetitive behaviours (Association, 2013). In addition, there is a growing body of evidence showing that ASD is associated with substantial differences in gut microbiota composition, as well as symptoms of gastrointestinal dysfunction, such as altered bowel habits, bloating, abdominal pain and increased intestinal permeability (D'Eufemia et al., 1996; De Angelis et al., 2013; Kang et al., 2013; McElhanon et al., 2014; Tomova et al., 2015; Luna et al., 2017; David, 2021; David et al., 2021; Fouquier et al., 2021). Overall, these findings indicate a disturbed communication between the gastrointestinal microbiota and the brain, the microbiota-gut-brain axis may be playing a role in some of the symptoms of ASD (Rhee et al., 2009; Collins et al., 2012; Cryan and Dinan, 2012; Mayer et al., 2014; Foster et al., 2017; Cryan et al., 2019; Sherwin et al., 2019). As such, the gut microbiome is increasingly being recognised as an important novel player and therapeutic target in ASD (Vuong and Hsiao, 2017). This is additionally supported by a study showing that the transplantation of standardised human gut microbiota to ASD-diagnosed children resulted in improved gastrointestinal functionality and reduced behavioural ASD scoring (Kang et al., 2019a,b).

Preclinical research has proven crucial in finding microbiota-based therapeutics for ASD (Hsiao et al., 2013; Kumar and Sharma, 2016). A preclinical animal model often used to study ASD is the BTBR T^{+} $Itpr3^{tf}$/J mouse strain. As is the case for humans, this mouse model shows robust deficits in social interaction, increased repetitive behaviours, altered immunity, and an abnormal gut microbiota accompanied by symptoms of gastrointestinal dysfunction (Moy et al., 2007; Coretti et al., 2017; Golubeva et al., 2017; Sgritta et al., 2019; Sharon et al., 2019; O'Connor et al., 2021). A novel modulator of the microbiota-gut-brain axis is the traditionally fermented milk drink kefir (Bourrie et al., 2016; Aslam et al., 2020). This milk drink is fermented by a community of bacteria and yeasts that stably coexist through metabolic cooperation and uneven partitioning between kefir grain and milk (Blasche et al., 2021). Previous work from our laboratory has demonstrated that kefir can modulate the microbiota and decrease repetitive behaviour in the most commonly used C57BL/6 mouse strain (van de Wouw et al., 2020b). In addition, a probiotic containing kefir-derived bacteria ameliorates lipopolysaccharide-induced changes in immune responses and depression- and anxiety-like behaviours (Murray et al., 2019), while kefir-derived peptides have been shown to reduce depression-like behaviours (Chen et al., 2021). As such, we aimed to investigate if kefir supplementation could ameliorate some of the ASD deficits observed in the BTBR T^{+} $Itpr3^{tf}$/J mouse strain, such as social interaction, repetitive behaviour and gastrointestinal function. Furthermore, we aimed to interrogate the peripheral immune system as a key mediator of kefir-induced gut-brain communication (Lowry et al., 2016; Langgartner et al., 2019) and investigate if any of these changes correlated with alterations in the neuroactive capacity of the microbiome.

2. Methodology

2.1. Animals

This study used male BTBR T^{+} $Itpr3^{tf}$/J mice (5–6 months of age at the start of the experiment, inhouse bred). Animals were housed as three mice per cage, with one cage containing two animals. As such, treatment groups were divided into Milk control (n = 11), and Kefir UK4 (n = 9). The holding room had a temperature of 21 ± 1°C and humidity of 55 ± 10% with a 12-hour light/dark cycle (lights on at 7:00 am). Food and drinking water were provided *ad libitum* throughout the study. Bodyweight was monitored weekly. All experiments were conducted under the project authorization license B100/3774 in accordance with the European Directive 86/609/EEC and the Recommendation 2007/526/65/EC and were approved by the Animal Experimentation Ethics Committee of University College Cork. All efforts were made to reduce the number of animals used and to minimise the suffering of the animals.

2.2. Experimental timeline and behavioural testing

Animals received daily kefir administration by oral gavage for three weeks prior to the assessment of their behavioural phenotype using various tests, which were formed in order of least stressful to most stressful to reduce the likelihood of prior behavioural tests influencing subsequent ones (Fig. 1). In addition, there was a minimum of 36-hours between tests. Behavioural testing started at 9 a.m. The order of testing was as follows: 1) Open field test, 2) Marble burying test, 3) Assessment of self-grooming, 4) 3-Chamber social interaction test, 5) Elevated plus maze, 6) Tail-suspension test, 7) Stress-induced hyperthermia test, 8) Intestinal motility test, 9) FITC-Dextran intestinal permeability test, 10) Fear conditioning, 11) Forced swim test. At the end of the study, animals were sacrificed by decapitation.

2.3. Kefir culturing and administration

Kefir UK4 was chosen based on its ability to decrease repetitive behaviour and modulate adaptive immunity (van de Wouw et al., 2020b). Kefir grains were cultured in Irish whole full fat cow's milk (2% w/v) at 25°C and milk was renewed every 24 h using a sterile Buchner funnel and sterile Duran bottle, as previously described (Dobson et al., 2011; Walsh et al., 2016). Grains were rinsed with sterile deionised water prior to the renewal of milk. The fermented milk (i.e., kefir) collected after the culturing, or milk control, was administered to the mice within one hour by oral gavage (0.2 mL). Daily kefir administration was performed between 4.00 and 7.00 p.m, which was after the behavioural test if one was performed that day.

2.4. Open field test

Mice were assessed for locomotor activity and response to a novel environment in the open field test, which was conducted as previously described (Burokas et al., 2017). Animals were placed in an open arena (40×32×24 cm, L × W × H) and were allowed to explore the arena for 10 min. Animals were habituated to the room 30 min prior to the test. Testing was performed under dim light (60 lx). The open field test box was cleaned with 70% ethanol in-between animals. Experiments were videotaped using a ceiling camera and were analysed for time spent in the virtual centre zone (defined as 50% away from the edges) and total distance travelled using Ethovision version 13 software (Noldus).

2.5. Marble burying test

Mice were tested for repetitive and anxiety-like behaviour with the marble burying test, which was conducted as previously described (Burokas et al., 2017). Animals were individually placed in a novel Plexiglas cage (35×28×18.5 cm, L × W × H), which was filled with sawdust (5 cm) and had 20 equally spread marbles placed on top (5×4 rows). After mice had spent 20 min in the cage, the number of buried marbles was counted by two researchers and averaged. A buried marble was defined as 2/3 of the marble not being visible anymore. In addition, all experiments were videotaped using a ceiling camera and the time the mice showed burying behaviour was scored. Sawdust was renewed, and marbles cleaned with 70% ethanol in-between animals.

2.6. Self-grooming test

Mice were tested for repetitive and anxiety-like behaviour by assessing self-grooming. Animals were individually placed in a 250 mL glass beaker for 30 min. A hard-plastic cover was put on the beaker to

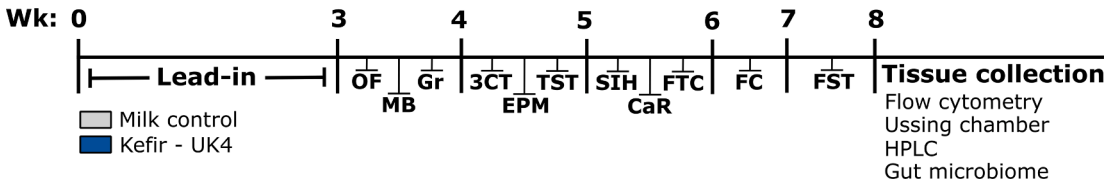

Fig. 1. Experimental design. After three weeks of treatment lead-in, animals were assessed for their behavioural phenotype. Treatment groups consisted of: Milk control (n = 11) Kefir – UK4 (n = 9). The order of behavioural tests was as follows; Week 3: Open field test (OF), Marble burying test (MB), Grooming test (Gr); Week 4: 3-Chamber social interaction test (3CT), Elevate plus maze (EPM), Tail suspension test (TST); Week 5: Stress-induced hyperthermia test (SIH), Carmine red intestinal motility test (CaR), FITC-Dextran intestinal permeability test (FTC); Week 6: Fear conditioning (FC); Week 7: Forced swim test (FST); Week 8: Postmortem, the immune system was assessed by flow cytometry, *ex vivo* intestinal permeability was tested on ileal and colonic tissue using ussing chambers, ileum and colonic serotonergic levels were quantified by high-performance liquid chromatography (HPLC), and the gut microbiome was analysed using metagenomic shotgun sequencing. (For interpretation of the references to colour in this figure legend, the reader is referred to the web version of this article.)

prevent the mice from escaping and paper covers were put between the beakers containing test mice to block visual contact. This test was performed under dim light (60 lx). All experiments were videotaped using a camera and scored for grooming time. Beakers and the hard-plastic cover were cleaned after each test mouse with 70% ethanol and left to dry for a few minutes.

2.7. Three-chamber social interaction test

The three-chamber sociability test was used to assess social preference and recognition and was conducted as previously described (Desbonnet et al., 2014). The testing apparatus was a three-chambered, rectangular box. The dividing walls between each chamber (20×40×22 cm, L × W × H) had small circular openings (5 cm diameter), allowing for access to all chambers. The two outer chambers contained wire cup-like cages (10 cm bottom diameter, 13 cm height), allowing for auditory, olfactory and visual, but no physical contact. The test consisted of 10-minute three phases: 1) Habituation, 2) Social preference, 3) Social recognition. In the first phase (Habituation), mice were allowed to explore the entire box with both wire cup-like cages left empty to allow for habituation to the novel environment. In the second phase (Social preference), one wire cup-like cage contained a novel, age-matched, conspecific, male mouse, whereas the other cage contained an object (rubber duckie). In the third phase (Social recognition), the mouse of the previous trial was left in the wire cup-like cage (Familiar mouse), while the object was replaced with a conspecific mouse (Novel mouse). The test mouse was held in the middle chamber while the conspecific mouse and object were placed in the cup wire-like cages. The location of the conspecific mice and object were systemically altered in-between test mice. The three-chamber test apparatus and wire cup-like cages were cleaned with 70% ethanol after each test mouse and left to dry for a few minutes. The three-chamber test apparatus was not cleaned with 70% ethanol in between testing phases. To reduce potential anxiogenic factors, all mice were habituated to the testing room 40 min before the test, the floor of the testing arena was covered with sawdust and testing was performed under dim light (60 lx). All experiments were videotaped using a ceiling-mounted camera and were scored blinded for the time interacted with the wire cup-like cages. The discrimination index was calculated as follows: Time spent interacting with object or mouse/Total time spent interacting *100%.

2.8. Elevated plus maze

The elevated plus maze test was used to assess anxiety-like behaviour and was conducted as previously described (Burokas et al., 2017). The elevated plus maze apparatus was elevated 1 m above the ground and consisted of a grey cross-shaped maze with two open arms and two closed arms (50×5 cm with 15 cm walls in the closed arms and 1 cm walls in the open arms). Mice were allowed to explore the maze for 5 min. Mice were habituated to the room 30 min prior to the test. Experiments were conducted in red light (5 lx). The elevated plus maze apparatus was cleaned with 70% ethanol in-between animals. Experiments were videotaped using a ceiling-mounted camera and videos were scored blinded for time spent in the open arms, which was defined as all paws in the open arm.

2.9. Tail-suspension test

The tail-suspension test was used to assess depressive-like behaviour and was conducted as previously described (Burokas et al., 2017). Mice were hung by their tail using adhesive tape (2 cm from the tip of the tail) to a 30 cm-elevated grid bar for 6 min. Experiments were videotaped using a numeric tripod-fixed camera and videos were scored blinded for the time mice spent immobile.

2.10. Stress-induced hyperthermia test

The stress-induced hyperthermia test was used to assess stress-responsiveness, which was conducted as previously described (Burokas et al., 2017). Body temperature was determined at baseline (T1) and 15 min later (T2) by gently inserting a Vaseline-covered thermometer 2.0 cm into the rectum. The temperature was noted to the nearest 0.1°C after it stabilised (~10 s). Mice were restrained by scruffing during this procedure which was the stressor. Animals were habituated to the testing room 1 h prior to the test. The difference between T1 and T2 reflected stress-induced hyperthermia.

2.11. Intestinal motility assay

Gastrointestinal motility was assessed as previously described (Golubeva et al., 2017). Briefly, mice were single-housed at 8.00 a.m. with *ad libitum* access to food and drinking water. Three hours later, 0.2 mL of non-absorbable 6% carmine red in 0.5% methylcellulose dissolved in sterile phosphate-buffered saline was administered by oral gavage, after which drinking water was removed. The latency for the excretion of the first red-coloured faecal pellet was subsequently timed as a measure of gastrointestinal motility.

2.12. Assessment of faecal water content and weight

Mice were single-housed for one hour during which faecal pellets were collected (±9 per animal). Pellets were subsequently weighed, incubated at 50°C for 24 h and weighed again. The average weight per pellet and percentage of faecal water content was calculated. In addition, on a separate day, animals were single housed prior to the start of the active-phase for 24-hours. Faecal pellets from the entire cage were subsequently collected and animals were placed back into their original housing cages.

2.13. FITC-Dextran intestinal permeability test

Gastrointestinal permeability was assessed using the FITC-dextran

intestinal permeability test, which was conducted as previously described (van de Wouw et al., 2018). Mice were fasted overnight and received an oral gavage of FITC-dextran dissolved in sterile PBS (Sigma, FD4) at 9 a.m. The administered dosage was 600 mg/kg body weight, and the approximate volume administered per mouse was 0.21 mL. Two hours after the FITC-dextran was administered, approximately 50 µl of whole blood was taken by tail-tip. For this procedure, the end of the tail was held with two fingers without restraining the mouse. A 2–4 mm long diagonal incision was made at the end of the tail using a single edge razor blade, and blood was collected in an EDTA-containing capillary. Blood was then transferred to a tube, centrifuged for 15 min at 3.500 g at 4°C, and plasma was collected and stored at −80°C for later analysis. Plasma FITC-dextran concentrations were assessed with a multi-mode plate reader (Victor 3, Perkin Elmer) with an excitation of 490 nm and emission of 520 nm.

2.14. Fear conditioning

Fear conditioning was used to assess amygdala-dependent learning memory and was conducted as previously described (Izquierdo et al., 2006). The test consisted of 3 days/phases; 1) Training, 2) Assessment of cued memory, 3) Assessment of contextual memory, each of which was carried on successive days with a 24-hour interval. In phase 1 (training), animals were recorded for 3 min (baseline), followed by 6 tone-conditioned stimuli (70 dB, 20 s), followed by a foot shock (0.6 mA, 2 s), with a 1-minute interval. In phase 2 (Assessment of cued memory), mice were placed in a novel context (i.e. black-checkered walls with a solid Plexiglas opaque floor, under which paper was placed containing a 400 µl vanilla solution (79.5% water/19.5% ethanol/1% vanilla-extract solution), and after an initial acclimation period of 2 min, mice received 40 presentations of the tone-conditioned stimuli, each lasting 30 s with a 5-second interval. In phase 3 (Assessment of contextual memory), mice were placed in the context of day 1 and recorded for 5 min, without the presentation of any tone-conditioned stimuli. The fear conditioning apparatus was cleaned with 70% ethanol in-between animals, but not between trials.

2.15. Forced swim test

The forced swim test was used to assess depressive-like behaviour and was conducted as previously described (Cryan and Mombereau 2004). Mice were individually placed in a transparent glass cylinder (24×21 cm diameter) containing 15-cm-depth water (23–25°C) for 6 min. Mice were gently dried after the test and water was renewed after each animal. Experiments were videotaped using a ceiling camera and videos were scored blinded for immobility time in the last 4 min of the test.

2.16. Repeated plasma sampling for corticosterone quantification

Plasma from each animal was sampled by tail-tip five minutes before the forced swim test, and repeatedly after the test in 30-min intervals up to 120 min. For the tail-tip, the end of the tail was gently held with two fingers without restraining the mouse. Using a single edge razor blade, a 2–4 mm long diagonal incision was made at the end of the tail. Approximately 40 µl of whole blood was taken per time point using an EDTA-containing capillary (Fisher Scientific, 749311), deposited in an Eppendorf and centrifuged for 10 min at 3500 g at 4°C. Plasma was collected and stored at −80°C for later corticosterone quantification.

2.17. Tissue collection

The collection of faecal samples throughout the study was done by single housing mice until 3 pellets were dropped between 10.00 and 12.00 a.m. The order of faecal pellet collection was counterbalanced between groups to minimise the effect of the circadian rhythm. Pellets were snap-frozen on dry ice within 3 min after excretion and subsequently stored at −80°C. Faecal pellets from week 8 were used for monoamine quantification using high-performance liquid chromatography (HPLC). The caecum contents collected when animals were sacrificed were used for the gut microbiome analysis.

Animals were sacrificed by decapitation in a random fashion regarding test groups between 9.00 a.m. and 2.00 p.m. Trunk blood was collected in EDTA-containing tubes and 100 µl was put in a separate Eppendorf for flow cytometry. Both tubes were centrifuged for 10 min at 3500 g at 4°C, after which plasma was collected and stored at −80°C for later analysis. The remaining cell pellet of the Eppendorf containing 100 µl blood was stored at 4°C and subsequently used for flow cytometry. Mesenteric lymph nodes (MLNs) were dissected, cleaned from fat tissue and stored in RPMI-1640 medium with L-glutamine and sodium bicarbonate (R8758, Sigma), supplemented with 10% FBS (F7524l, Sigma) and 1% Pen/strep (P4333, Sigma) at 4°C for subsequent flow cytometry. The caecum was weighed, snap-frozen on dry ice and stored at −80°C. The length of the colon was measured, and the proximal and distal 2 cm were collected and cut in half. One side was snap-frozen on dry ice and stored at −80°C and the other treated with RNAlater (Sigma, R0901). This was done by incubating the tissues for 48 h at 4°C, after which the RNAlater was removed and tissues were stored at −80°C for gene expression analysis. Whole brains were snap-frozen in ice-cold isopentane and stored at −80°C. For mucus staining, 1.5 cm of the distal colon was collected containing a faecal pellet to ensure the integrity of the mucus layer. The tissue was subsequently incubated in Carnoy's solution (100% ethanol, chloroform and glacial acetic acid in a ratio of 6:3:1) for 2 h at 4°C and subsequently stored in 100% ethanol at 4°C for paraffin embedding.

2.18. Intestinal permeability by Ussing chamber

This assay was used to assess ileal and colonic permeability *ex vivo* and was performed as previously described with minor modifications (Golubeva et al., 2017). A piece of distal ileum (1.5 cm segment taken 2.0 cm proximally from the caecum) and proximal colon (1.0 cm segment) were emptied of their contents, cleaned and put in Krebs buffer (1.2 mM NaH_2PO_4, 117 mM NaCl, 4.8 mM KCl, 1.2 mM $MgCl_2$, 25 mM $NaHCO_3$, 11 mM $CaCl_2$ and 10 mM glucose). The samples were mounted within 5 min in Ussing chambers with an exposed tissue area of 0.12 cm^2. No seromuscular stripping was performed. The permeability of the epithelial layer was measured via paracellular flux of 4 kDa FITC-dextran (Sigma-Aldrich, FD4). FITC-dextran was added to the mucosal chamber at a final concentration of 2.5 mg/mL. To assess serosal-to-mucosal FITC flux across the epithelium, 200 µl was collected from the serosal chamber at baseline and after 60, 90 and 120 min. FITC absorbance was measured at 485 nm excitation/535 nm emission wavelengths through fluorometric analysis using a multi-mode plate reader (Victor 3, Perkin Elmer). FITC flux was then calculated as an increment in fluorescence intensity vs baseline fluorescence in the serosal compartment and presented in ng/mL.

2.19. Flow cytometry

Flow cytometry was performed as previously described (Gururajan et al., 2019; van de Wouw et al., 2020a). Blood analysed using flow cytometry was collected prior to the forced-swim test, as well as 30 and 120 min following it. MLNs were collected when animals were sacrificed. All samples were processed on the same day for flow cytometry. Blood was resuspended in 10 mL home-made red blood cell lysis buffer (15.5 mM NH_4Cl, 1.2 mM $NaHCO_3$, 0.01 mM tetrasodium EDTA diluted in deionised water) for 3 min. Blood samples were subsequently centrifuged (1500 g, 5 min), split into 2 aliquots and resuspended in 45 µl staining buffer (autoMACS Rinsing Solution (Miltenyi, 130-091-222) supplemented with MACS BSA stock solution (Miltenyi, 130-091-376)) for the staining procedure. MLNs were poured over a 70 µm strainer

and disassembled using the plunger of a 1 mL syringe. The strainer was subsequently washed with 10 mL media (RPMI-1640 medium with L-glutamine and sodium bicarbonate, supplemented with 10% FBS and 1% Pen/strep), centrifuged and $1x10^6$ cells were resuspended in 45 µl staining buffer for the staining procedure. For the staining procedure, 5 µl of FcR blocking reagent (Miltenyi, 130-092-575) was added to each sample. Samples were subsequently incubated with a mix of antibodies (Blood aliquot 1; 5 µl CD11b-VioBright FITC (Miltenyi, 130-109-290), 5 µl LY6C-PE (Miltenyi, 130–102-391), 0.3 µl CX3CR1-PerCP-Cyanine5.5 (Biolegend, 149010) and 5 µl CCR2-APC (Miltenyi, 130–108-723 MLNs; 1 µl CD4-FITC (ThermoFisher, 11-0042-82) and 1 µl CD25-PerCP-Cyanine5.5 (ThermoFisher, 45-0251-80)) and incubated for 30 min on ice. Blood samples were subsequently fixed in 4% PFA for 30 min on ice and MLNs underwent intracellular staining using the eBioscience™ Foxp3/Transcription Factor Staining Buffer Set (ThermoFisher, 00-5523-00), according to the manufacturers' instructions, using antibodies for intracellular staining (2 µl FoxP3-APC (ThermoFisher, 17-5773-82) and 5 µl Helios-PE (ThermoFisher, 12-9883-42)). Fixed samples were resuspended in staining buffer and analysed the subsequent day on the BD FACSCalibur flow cytometry machine. Data were analysed using FlowJo (version 10). The investigated cell populations were normalised to PBMC levels.

2.20. Plasma corticosterone and cytokine assessment

Corticosterone quantification of plasma samples (20 µl) obtained in the forced swim test was performed using a corticosterone ELISA (Enzo Life Sciences, ADI-901-097) according to the manufacturer's guidelines. Plasma adrenaline and noradrenaline were quantified using an ELISA (Abnova, KA1877) according to the manufacturer's instructions with one minor modification, where 15 µl plasma was used instead of 300 µl. Absorbance was read using a Biotek Synergy H1 plate reader equipped with Gen5 software (Biotek, Winooski, VT, USA). Cytokine levels from plasma samples collected during euthanasia were quantified using the V-PLEX Proinflammatory Panel 1 Mouse Kit (MSD, K15048D). Cytokine quantification was done according to the manufacturer's guidelines with one modification, where 20 µl plasma sample was added onto the plate and incubated overnight (15 h) at 4°C, after which the rest of the protocol was carried out as suggested by the guidelines. Values under the fit curve range and detection range were excluded.

2.21. Colonic mucus layer staining

Colonic samples were embedded in paraffin with a histokinette (Leica TP1020 Tissue Processor) using the following program: 100% ethanol – 90 min; 50% ethanol/50% histoclear – 60 min; 2 cycles 100% histoclear – 120 min; 2 cycles 100% paraffin at 60°C – 120 min. Tissues were subsequently cut in half, oriented for transversal sectioning and embedded in paraffin blocks using the Tissue-Tek® TEC™ 5 apparatus (Sakura). Samples were sectioned (8 µm) using the rotary microtome Leica RM2135 and left to dry at 50°C for 24 h.

Sections were stained with alcian blue and periodic acid for the mucus layer, with Nuclear fast red as a counterstain. Briefly, histolene – 10 min; 2 cycles 100% ethanol – 5 min; 95% ethanol – 5 min; 70% ethanol – 5 min; tap water – 10 min; 3% acetic acid – 3 min; 1% alcian blue (Sigma Aldrich, 8GX. Acian blue was dissolved in 3% acetic acid, stirred overnight, brought to a pH of 2.5, and filtered) – 30 min; 3% acetic acid – 10 sec; tap water – 2 min; distilled water – one rinse; 0.5% periodic acid (Acros Organics, A0374808) – 5 min; distilled water – one rinse; Schiff's reagent (Fisher Scientific, 1713072) – 10 min; tap water – 5 min; Nuclear fast red (Sigma Aldrich, N3020) – 5 min; tap water – 1 min; 95% ethanol – 3 min; 100% ethanol – 3 min; 100% ethanol – 3 min. Finally, sections were covered with a cover-slip using DPX mounting.

Pictures were taken using full-bright microscopy (Olympus BX51 brightfield Microscope) and analysed using. The mucus thickness (µm) was subsequently measured using ImageJ2 software. As mucus thickness measurements of the same animal were quite variable between different pictures, we chose to take 81 measurements per animal. Specifically, 3 pictures were made of each of 9 different sections, after which 3 measurements were taken of each picture. These 81 measurements were non-normally distributed, so the median was taken of all measurements, which represented the colonic mucus thickness of that animal.

2.22. High-performance liquid chromatography

5-hydroxytryptamine (5-HT) and 5-hydroxyindoleacetic acid (5-HIAA) concentrations were determined using HPLC based on the methodology previously described (Clarke et al., 2013). Briefly, mobile phase consisted of HPLC-grade 0.1 M citric acid, 0.1 M sodium dihydrogen phosphate monohydrate, 0.01 mM EDTA disodium salt (Alkem/Reagecon), 5.6 mM octane-1-sulphonic acid (Sigma Aldrich), and 9% (v/v) methanol (Alkem/Reagecon). The pH of the mobile phase was adjusted to 2.8 using 4 N sodium hydroxide (Alkem/Reagecon). Homogenization buffer consisted of mobile phase with the addition of 20 ng/20 µl of the internal standard, N-methyl 5-HT (Sigma Aldrich). Briefly, tissue samples were sonicated (Sonopuls HD 2070) for 4 s in 500 µl cold homogenization buffer during which they were kept chilled. Tissue homogenates were then centrifuged at 14,000g for 20 min at 4°C. The supernatant was collected and the pellet was discarded. The supernatant was then briefly vortexed and 30 µl of supernatant was spiked into 270 µl of mobile phase. 20 µl of the 1:10 dilution was injected into the HPLC system (Shimadzu, Japan) which was comprised of a SCL 10-Avp system controller, LC-10AS pump, SIL-10A autoinjector, CTO-10A oven, LECD 6A electrochemical detector, and Class VP-5 software. The chromatographic conditions were flow rate of 0.9 mL/min using a Kinetex 2.6u C18 100A × 4.6 mm column (Phenomenex), oven temperature of 30°C, and detector settings of +0.8 V. 5-HT and 5-HIAA external standards (Sigma Aldrich, H7752 and H8876, respectively) were injected at regular intervals during sample analyses. Monoamines in unknown samples were determined by their retention times compared to external standards. Peak heights of the analyte: internal standard ratio were measured and compared with external standards, results were expressed as µg of neurotransmitter per gram of tissue.

2.23. Gut microbiome analysis

Metagenomic DNA was extracted from cecal contents using the QiaAmp PowerFecal Pro DNA Kit as per the manufacturer's instructions. Whole-metagenome shotgun libraries were prepared using the Nextera XT kit in accordance with the Nextera XT DNA Library Preparation Guide from Illumina and sequenced on the Illumina NextSeq 500 with a NextSeq 500/550 High Output Reagent Kit v2.5 (300 cycles). All sequencing was performed at the Teagasc Moorepark sequencing facility in accordance with standard Illumina protocols.

Adapter removal and quality trimming were performed using TrimGalore (v0.6.0) (https://github.com/FelixKrueger/TrimGalore), a wrapper script for Cutadapt (v2.6) and FastQC (v0.11.8), using default parameters (Andrews 2010, Martin 2011). Resulting reads were aligned to the C57BL/6NJ genome with Bowtie2 (v2.3.4), aligned reads were removed with samtools (v1.9), and converted from BAM to fastq format with bedtools (v2.27.1) (Langmead and Salzberg, 2012; Li et al., 2009a; Quinlan and Hall, 2010). Interleaved fastq files were generated using BBMap (v.38.22) (https://sourceforge.net/projects/bbmap/). Compositional and functional profiling was carried out with HUMAnN3 (v3.0) using ChocoPhlAn nucleotide database v30, uniref90 protein database, and MetaPhlAn3 database version v30 (Beghini et al., 2020). The resulting gene family and pathway abundance tables were sum-normalised to copies per million reads (CPM) to facilitate comparisons between samples with different sequencing depths. All downstream microbiome analysis, data manipulation, and plotting were performed in R (v. 4.0.2) using the 'tidyverse' package unless otherwise stated (Wickham et al., 2019). Shannon, Simpson, and Inverse Simpson indices

of alpha diversity, along with Bray-Curtis, Jaccard, and Chao indices of beta diversity, were calculated using the 'vegan' package (Oksanen et al., 2020). Phylogentic diversity and species richness were calculated using the 'picante' package, and UniFrac distances were calculated using the 'GUniFrac' package (Kembel et al., 2010; Chen et al., 2012). Differentially abundant metagenomic features were identified using the LEfSe Galaxy instance (https://huttenhower.sph.harvard.edu/galaxy/) and associations between metagenomic data and mouse behavioural and immunological were calculated by HAllA (v0.8.17) (Rahnavard et al., n. d.; Segata et al., 2011). Gut-Brain Modules were calculated by remapping HUMANn3 UniRef90 gene families to KEGG Orthologues using the packaged humann_regroup_table function, renormalised to CPM reads using the humann_renorm_table function, and mapped to GBMs using Omixer-RPM (v1.1) (Darzi et al., 2016; Valles-Colomer et al., 2019).

To recover metagenome-assembled genomes (MAGs), group-specific metagenomic co-assemblies were constructed with metaSPAdes (v. 3.14) and paired-end fastq reads were aligned to these by Bowtie2 with default parameters (Nurk et al., 2017). The resulting SAM files were converted to BAM format and sorted using Samtools, and contig depth was calculated using the jgi_summarise_bam_contig_depths script bundled with MetaBat2 (v. 2.12.1) (Kang et al., 2019a). MetaBat2 was also used for contig binning and the lineage_wf workflow of CheckM (v. 1.0.18) was used to evaluate the quality of metagenomic bins (Parks et al., 2015). Only bins with completeness $\geq$ 90% and contamination <5% were considered "high quality" and retained for downstream analyses. These high-quality MAGs were taxonomically classified using PhyloPhlAn3 (v3.0) using the SGB.Dec19 database and functionally annotated by Prokka (v1.14) and the online instance of eggnog-mapper with default parameters (http://eggnog-mapper.embl.de/) (Seemann, 2014; Huerta-Cepas et al., 2017, 2019; Asnicar et al., 2020).

Mouse caecal metagenomic data (Milk control and kefir-UK4 groups) from a previous study (van de Wouw et al., 2020b), using this kefir were processed using the same method for adapter removal, quality trimming, host read removal, and taxonomic and functional profiling as used in the current study. Differentially abundant features from the previous study were identified by LEfSe and both datasets were processed together using Maaslin2 to identify patterns across both, while controlling for study (i.e., this study versus the previous one).

2.24. Statistical analysis

All behavioural and physiological data were assessed for normality using the Shapiro-Wilk test and Levene's test for equality of variances. The effect of kefir was determined by an unpaired Student's *t*-test when data were normally distributed and Mann-Whitney *U* test when data were non-normally distributed. Body weight and fear conditioning data were assessed using repeated-measures ANOVA. Statistical significance for social preference and recognition in the 3-chamber sociability test was assessed using Wilcoxon signed ranks test. Parametric data are depicted as bar graphs with points as individual data points and expressed as mean ± SEM. Non-parametric data is depicted as a box with whiskers plot. Statistical analysis was performed using SPSS software version 24 (IBM Corp). A p-value <0.05 was deemed significant.

3. Results

3.1. Kefir is well-tolerated in BTBR mice

No differences were found in body weight, locomotor activity or the weight of various adipose deposits between test and control mice throughout the study, indicating that kefir was well-tolerated in BTBR mice (sFig. 1**)**.

3.2. Kefir reduces repetitive behaviour in the marble burying test

Previous work from our lab has shown that BTBR mice have an enhanced engagement in repetitive behaviours in the marble burying test compared to C57BL/6 mice (Golubeva et al., 2017). Mice receiving kefir showed a trend towards decreased marbles buried ($t(17) = 2.104$, $p = 0.051$) (Fig. 2**A**). This was confirmed by measuring the time mice spent engaging in burying behaviour throughout this test ($U = 18$, $p = 0.033$) (Fig. 2**B**).

3.3. Kefir does not affect other measures of anxiety- and depressive-like behaviour

No differences were found in any of the other tests addressing anxiety-like behaviour, which included the assessment of self-grooming behaviour (sFig. 2**A**), the open field test (sFig. 2**B**), the elevated plus maze (sFig. 2**C**) and the stress-induced hyperthermia test (sFig. 2**D**). In addition, no changes were observed in any of the tests assessing depressive-like behaviour, like the tail suspension test (sFig. 2**E**) and forced swim test (sFig. 2**F**).

3.4. Mice receiving kefir show improvement of social recognition

Previous work from our lab has shown that BTBR mice show decreased social preference and recognition compared to C57BL/6 mice (Golubeva et al., 2017). Both mice receiving milk and kefir showed social preference (milk: ($t(10) = -3.995$, $p = 0.003$); kefir: ($Z = -1.956$, $p = 0.050$) (Fig. 3**A)**. No differences in the social preference ratio were observed (Fig. 3**B**). However, mice receiving milk only showed a trend towards social recognition ($Z = -1.778$, $p = 0.075$), while mice receiving kefir showed significance in social recognition ($Z = -2.073$, $p = 0.038$) (Fig. 3**C).** Nonetheless, no differences in the social recognition ratio were observed (Fig. 3**D**

3.5. Kefir does not affect fear-dependent learning and memory

Kefir administration does not influence fear-dependent learning, nor cued and contextual memory in the fear conditioning test (sFig. 3**A–D).**

3.6. Kefir ameliorates acute stress-induced LY6^{hi} monocyte alterations

BTBR mice have an increased corticosterone response to acute stress (Golubeva et al., 2017). This stress-induced increase in corticosterone, as well as catecholamines, is associated with a peripheral immune cell distribution, indicating immune cell trafficking (Dhabhar et al., 2012; van de Wouw et al., 2020a, 2021). We, therefore, investigated the corticosterone response to an acute stressor (i.e. forced swim test), where we observed that kefir prolonged stress-induced corticosterone increases at 60 min post-stress only ($U = 13$, $p = 0.009$) (Fig. 4**A**). No differences were observed in baseline levels of the catecholamine adrenalin and noradrenalin (Fig. 4**B and C**). We subsequently investigated changes in blood monocyte levels in response to stress. In line with previous reports (van de Wouw et al., 2020a), acute stress decreased blood LY6C^{hi} monocyte levels (CD11b+, LY6C^{hi} levels) ($F(2,59) = 72.243$, $p < 0.001$) (Fig. 4**E).** Interestingly, there was a trend towards an amelioration of this stress-induced effect in mice receiving kefir as detected by absolute levels of LY6C^{hi} monocytes ($t(18) = -1.819$, $p = 0.086$) (Fig. 4**E**), and relative decrease ($t(18) = 2.284$, $p = 0.035$) (Fig. 4**F).** Considering the pivotal role of the CCR2 receptor in LY6C^{hi} monocyte trafficking (Prinz and Priller 2010), we hypothesised that changes in CCR2 receptor expression could be underlying these acute stress-induced differences in LY6C^{hi} monocytes. Indeed, acute stress increased CCR2 receptor expression ($F(2,59) = 40.874$, $p < 0.001$) (Fig. 4**G**), and a trend towards decreased stress-induced increase in CCR2 receptor expression was observed in mice receiving kefir ($t(18) = -1.747$, $p = 0.098$) (Fig. 4**G**).

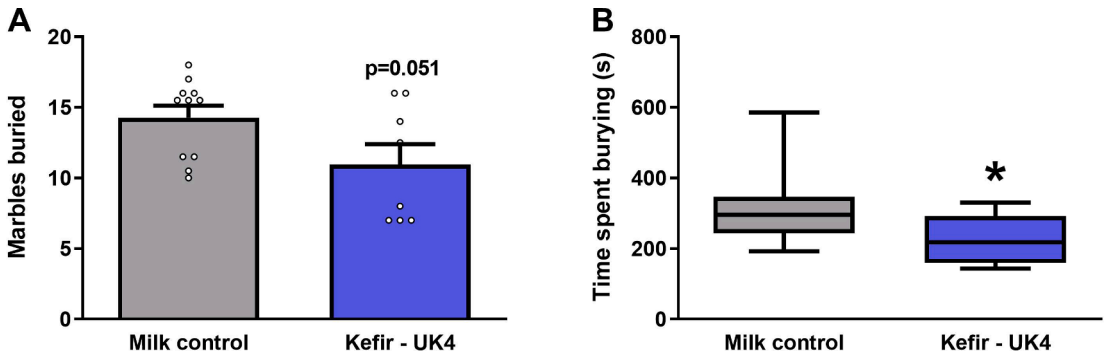

Fig. 2. Kefir decreased repetitive behaviour in the marble burying test. Animals were assessed for repetitive behaviour using the marble burying test. Both the number of marbles buried was quantified (A), as well as the time animals performed burying behaviour (B). The amount of marbles buried was normally distributed and analysed using an unpaired Student's *t*-test. The burying time was non-normally distributed and analysed using the Mann-Whitney *U* test. Significant differences are depicted as: *p < 0.05. All data are expressed as mean ± SEM or box-plot (n = 8–11). Dots on each graph represent individual animals.

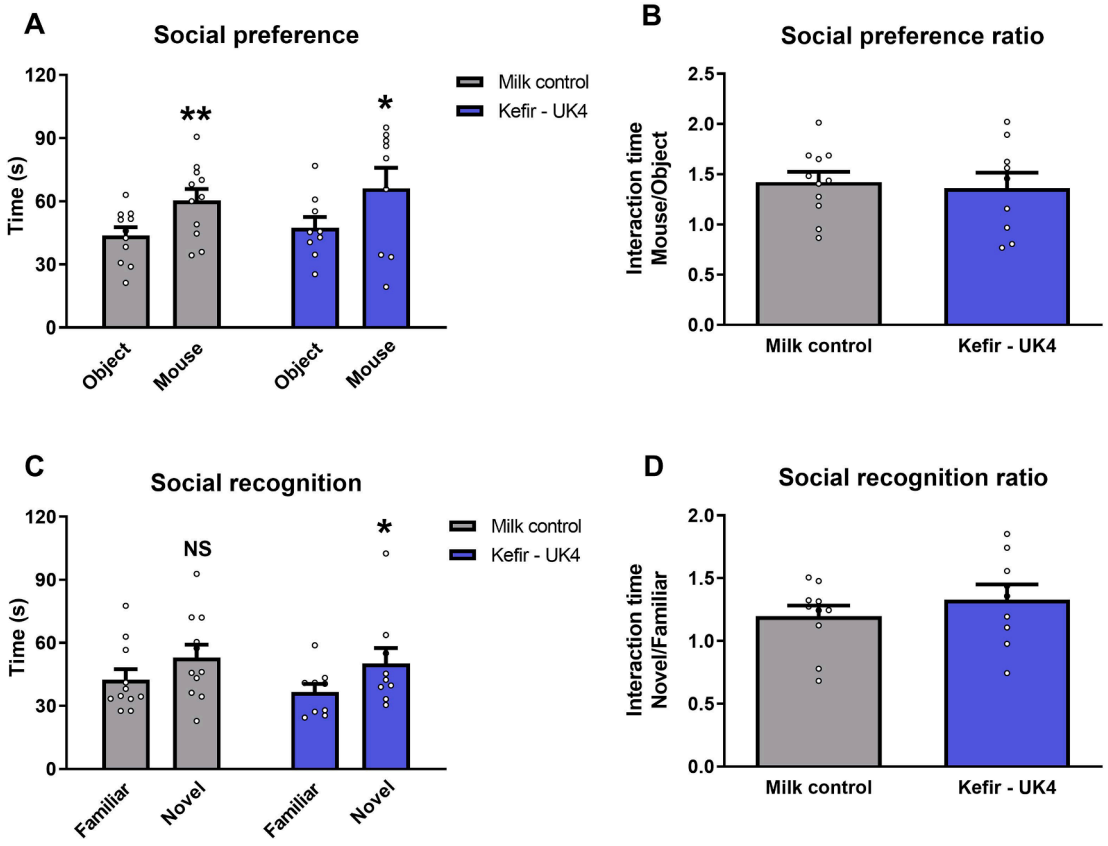

Fig. 3. All groups show social preference, while only mice receiving kefir show significant differences in social recognition. Social preference (A, B) and social recognition (C, D) were assessed using the 3-chamber social interaction test. All data were non-normally distributed and analysed using the Wilcoxon signed ranks test, except for social preference data for control mice, which were analysed using a paired Student's *t*-test. Significant differences are depicted as: *p < 0.05 and **p < 0.01. Data are expressed as either mean ± SEM (A, B) (n = 9–11). Dots on each graph represent individual animals.

3.7. Kefir increases T regulatory cells in mesenteric lymph nodes

Previous reports show that individuals with ASD, as well as BTBR mice have decreased CD4+, FoxP3+ cells, indicating decreased Treg cell levels (Ahmad et al., 2017; Bakheet et al., 2017). We found that kefir did not affect T helper cells (CD4+) levels in mesenteric lymph nodes (MLNs) (Fig. 5**B**), even though kefir did increase Treg cell (CD4+, CD25+, FoxP3+) levels (t(18) = -3.003, p = 0.008) (Fig. 5**C**). This increase in Treg cells could not be attributed to Treg cells specifically originating from the thymus (Helios+) or periphery (Helios-) (Fig. 5**D**). Surprisingly, even though a trend in decreased T helper cells (CD4+) was observed in the circulation (t(18) = 1.835, p = 0.083) (Fig. 5**E**), no corresponding changes were observed in circulating Treg cell counts (Fig. 5**F**). Furthermore, no differences were observed in plasma IL-10 levels, one of the primary cytokines secreted by Treg cells (Fig. 5**G**) (Sabat et al., 2010).

3.8. Kefir does not affect intestinal permeability

Considering previous work has shown that BTBR mice have decreased MUC2 mRNA expression in the colon, which is the primary constituent of the mucus layer, we wondered if kefir could influence the

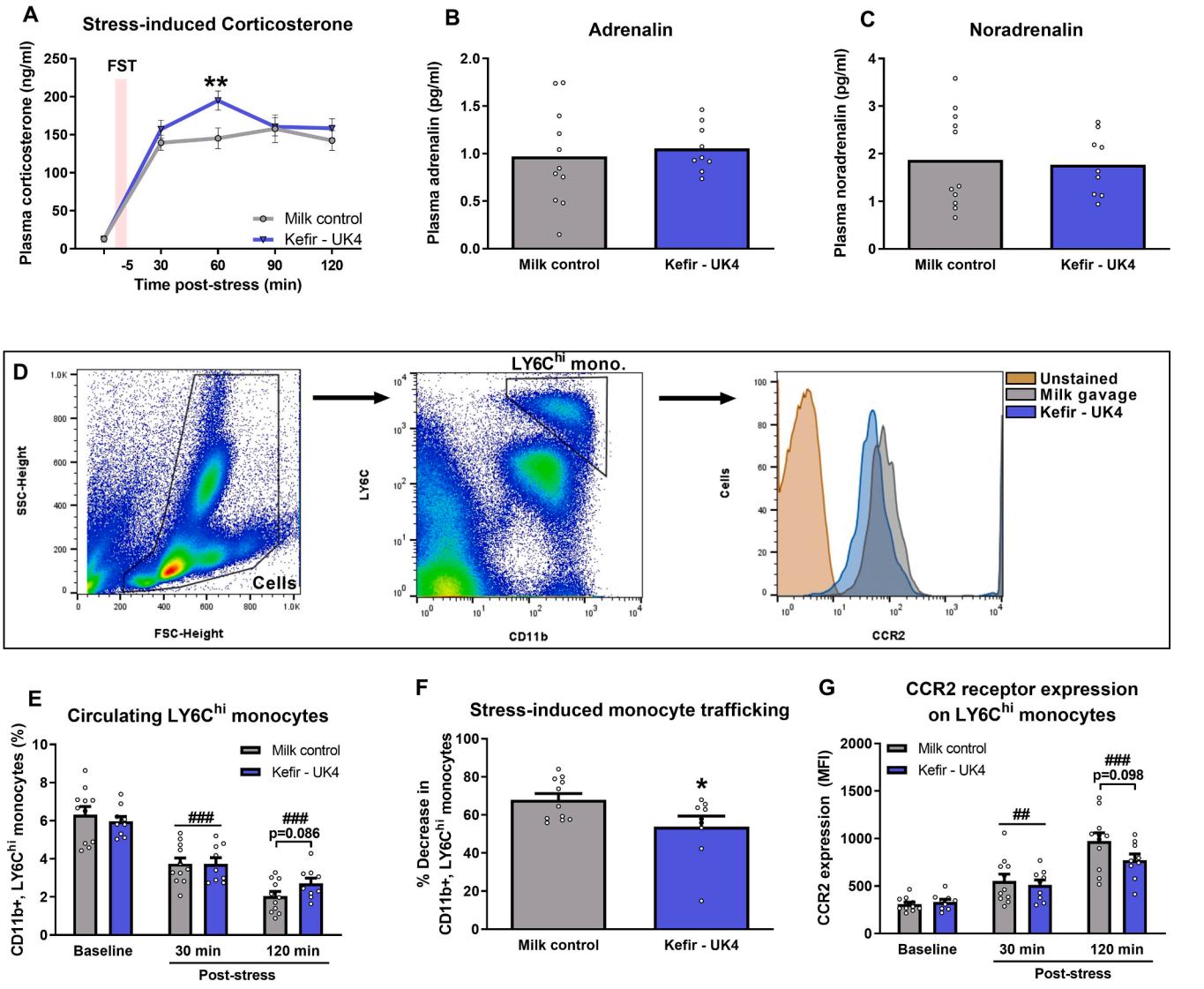

Fig. 4. Kefir increases stress-induced corticosterone responses yet ameliorates blood LY6C^{hi} monocyte changes. Plasma corticosterone levels were quantified before, and after forced swim test stress (A). Adrenalin and noradrenalin levels were quantified from plasma obtained when animals were sacrificed. For flow cytometry, cells were selected based on FSC-height and SSC-height. LY6C^{hi} monocytes were subsequently selected bas on CD11b and LY6C receptor expression, after which CCR2 receptor expression was quantified by assessing median fluorescent intensity (MFI). The histogram plot depicts CCR2 staining intensity of the representative samples of each group 120 min post-stress (D). Circulating LY6C^{hi} monocytes (CD11b+, LY6C^{hi}) were quantified at baseline, 30 min and 120 min post forced swim test stress (E). The relative decrease in LY6C^{hi} monocyte levels were subsequently calculated (F). And CCR2 expression (median fluorescent intensity – MFI) was quantified at baseline, 30 min and 120 min post-stress. All data were normally distributed. Stress effects were investigated using a one-way ANOVA following Dunnett post hoc correction. Kefir effects were analysed using an unpaired Student's *t*-test. Significant differences are depicted as: $^{\#\#}p < 0.01$ and $^{\#\#\#}p < 0.001$ for stress effects; $^{*}p < 0.05$ and $^{**}p < 0.01$ for kefir effects. All data are expressed as mean ± SEM (n = 9–11). Dots on each graph represent individual animals.

colonic mucus layer (Golubeva et al., 2017). However, kefir administration did not affect colonic mucus thickness (sFig. 4**A and B**). Similarly, it was previously reported that BTBR mice have increased epithelial permeability (Golubeva et al., 2017), which also remained unaffected by kefir treatment as measured *in vivo* (sFig. 4**C**), and *ex vivo* (sFig. 4**D and E**).

3.9. Kefir does not change gut serotonin levels and gastrointestinal motility

BTBR mice have previously been shown to have decreased 5-HT levels in the colon and ileum, as well as decreased intestinal motility compared to C57BL/6 mice (Golubeva et al., 2017). We hypothesised that kefir administration might ameliorate these deficits, but we did not observe any kefir-induced difference in ileal 5HIAA, 5-HT levels, as well as in the 5HIAA/5-HT ratio (sFig. 5**A–C**). In addition, no differences were present in colonic 5-HT levels and the 5HIAA/5-HT ratio (sFig. 5**E and F**), even though a trend was observed towards decreased 5HIAA levels ($U = 21$, $p = 0.062$) (sFig. 5**D**). Similarly, we did not observe any differences in gastrointestinal motility as determined by carmine red administration (sFig. 5**G**), average faecal pellet weight (sFig. 5**H**), faecal water content (sFig. 5**I**) and colon length (sFig. 5**J**). Interestingly, kefir UK4 did increase cecum weights ($U = 17$, $p = 0.017$) (sFig. 5**K**). Notably, previous work from our lab has shown that BTBR mice have no altered cecum weight compared to C57BL/6 mice (data not published).

3.10. Kefir increases Lachnospiraceae bacterium A2 and decreases Clostridiaceae abundance

It has previously been shown that BTBR mice have a reduced alpha diversity (Golubeva et al., 2017). Kefir administration did not significantly impact alpha or beta diversity of the caecal microbiome (Fig. 6**A**

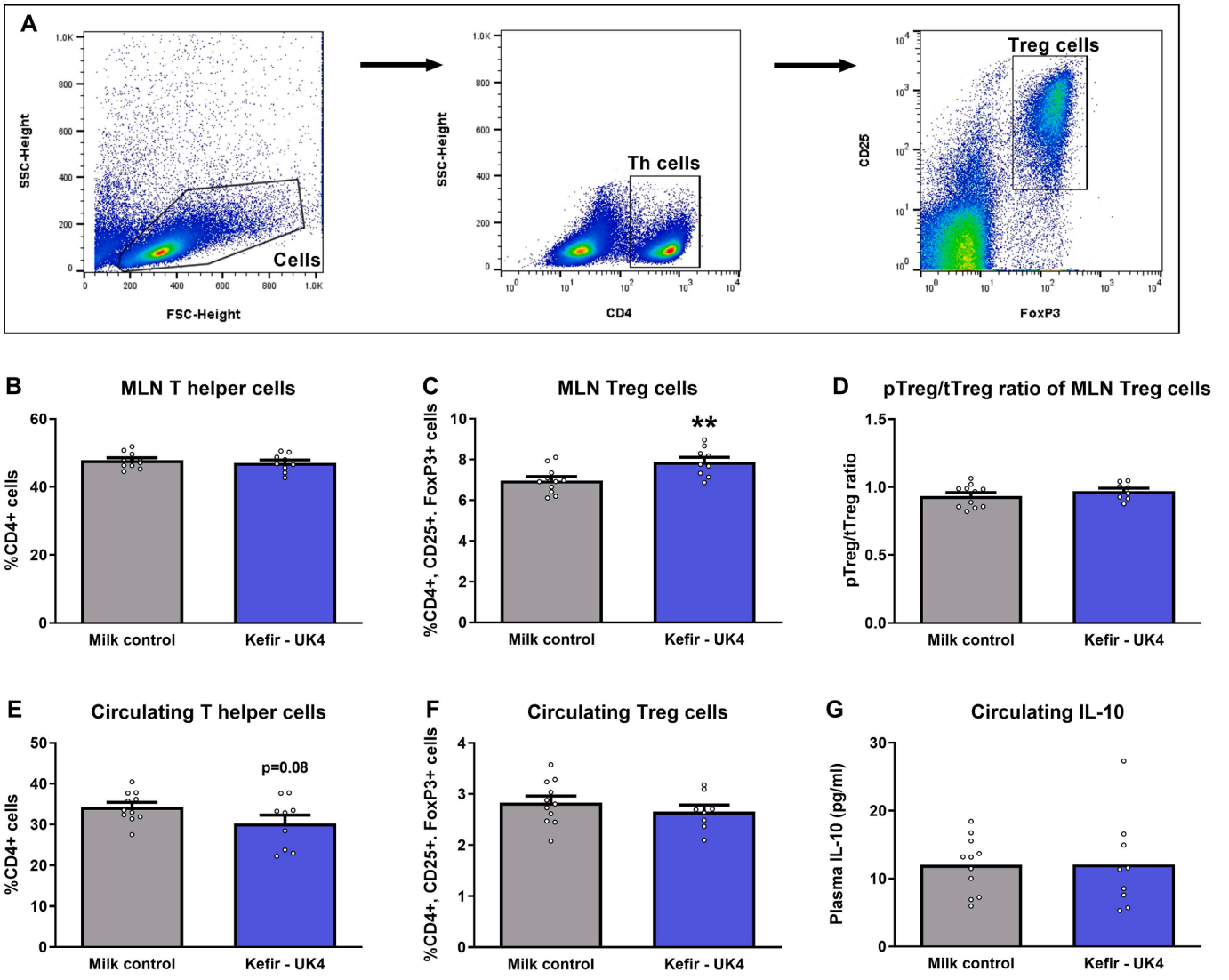

Fig. 5. Kefir increases MLN Treg cell, but not circulating Treg cell levels. Cells were selected based on FSC-height and SSC-height. T helper cells were subsequently selected based on CD4 receptor expressions and Treg cells finally were selected on CD25 receptor expression and FoxP3 transcription factor expression (A). T helper cells (CD4+) were quantified in mesenteric lymph nodes (MLNs) (B). In addition, Treg cell (CD4+, CD25+, FoxP3+) levels were quantified in MLNs (C). The origin (thymus vs periphery) of Treg cells were subsequently assessed by quantifying the expression of the transcription factor Helios (D). The same analyses were done for blood (E-G). All data were normally distributed and analysed using an unpaired Student's *t*-test. Significant differences are depicted as: **p < 0.01. All data are expressed as mean ± SEM (n = 9–11). Dots on each graph represent individual animals.

and B). However, kefir supplementation did increase the relative abundance of *Lachnospiraceae bacterium A2* (LDA = 4.60, p = 0.048), and reduced the relative abundance of the genus *Clostridium* and family *Clostridiaceae* (LDA = 4.25, p = 0.025; LDA = 4.25, p = 0.025, respectively) (Fig. 6**C**). *Lachnospiraceae bacterium A2* was not present in the administered kefir (van de Wouw et al., 2020b), and has not been identified as a component of the kefir microbiota by others.

3.11. Kefir modulates specific aspects of the predicted function of the microbiome

Kefir administration did not affect the overall predicted functionality of the gut microbiome as indicated by beta diversity (Fig. 7**A**). Subsequent investigation into differentially abundant pathways revealed 2 increased and 7 reduced pathways following kefir supplementation (Fig. 7**B**). The increased pathways include all-*trans*-farnesol biosynthesis and glycolysis (LDA = 3.15, p = 0.037; LDA = 2.50, p = 0.044 respectively), while the reduced pathways include L-rhamnose biosynthesis and degradation (LDA = 3.17, p = 0.037; LDA = 2.76, p = 0.044 respectively), three pathways involved in pyrimidine deoxyribonucleotides *de novo* biosynthesis and phosphorylation (LDA = 2.80, p = 0.037; LDA = 2.77, p = 0.030; LDA = 2.80, p = 0.017 respectively), and two pathways involved in galactose degradation (LDA = 2.95, p = 0.044; LDA = 2.95, p = 0.044 respectively). Subsequently, changes in the microbiome were explored in the context of the gut-brain axis by examining the abundances of gut-brain modules (GBMs), which are groups of KEGG Orthogroups (KOs) that are associated with the production of neuroactive compounds (Valles-Colomer et al., 2019; van de Wouw et al., 2020b; Boehme et al., 2021). Only the GBM S-adenosylmethionine synthesis was increased following kefir administration (Fig. 7**C**).

We investigated differentially abundant pathways associated with the bacterial taxon that was differentially abundant following kefir supplementation. The increased relative abundance of *L. bacterium A2* was accompanied by an increase in 28 pathways encoded by this species (Fig. 7**D**). Furthermore, *L. bacterium A2* contained genes encoding for 9 GBMs, one of which was SAM (sTable 1).

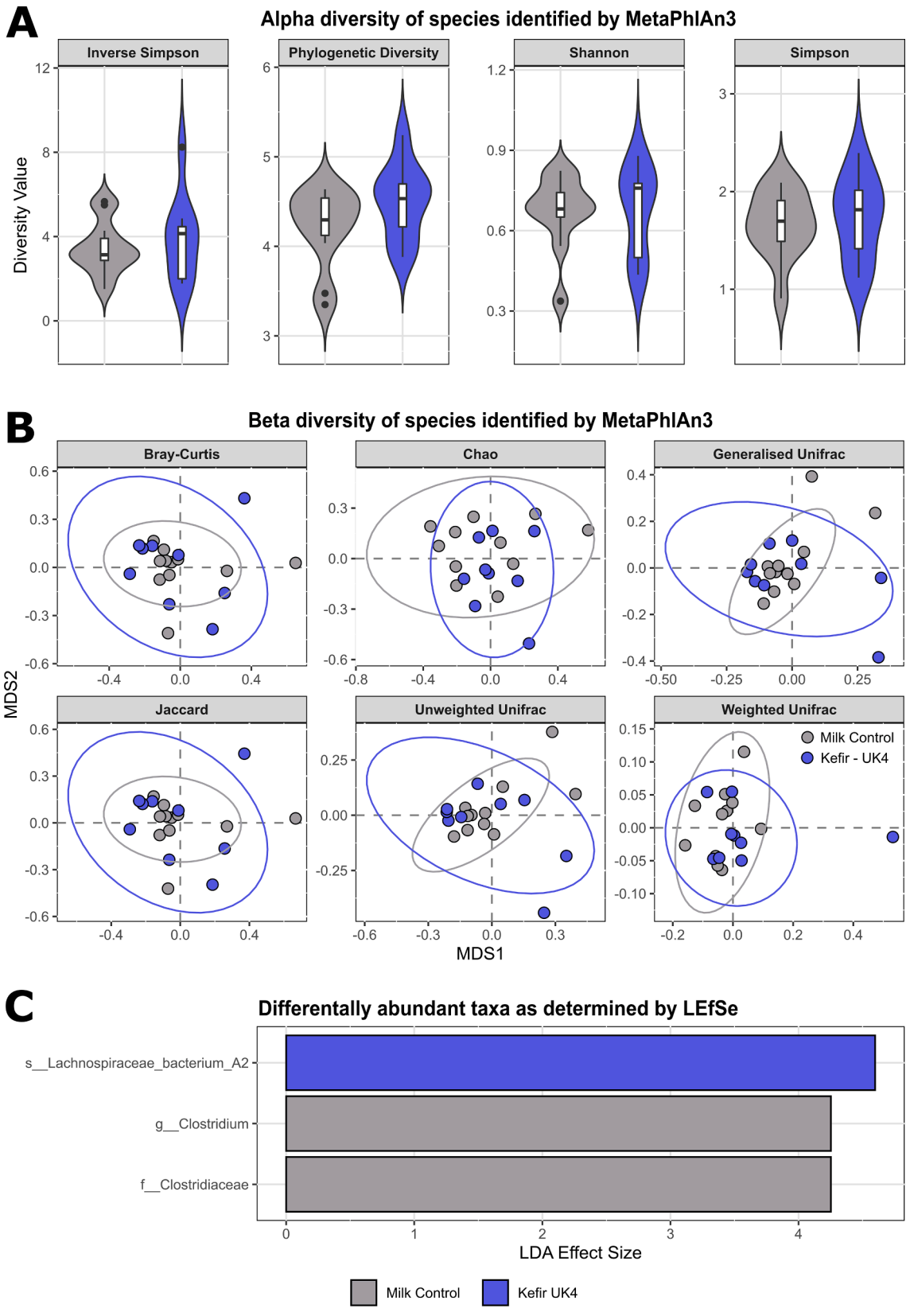

Fig. 6. Kefir increases *Lachnospiraceae bacterium A2* and decreases Clostridiaceae abundance without altering alpha and beta diversity. Alpha diversity investigated using inverse Simpson, phylogenetic diversity, Shannon and Simpson indices (A). Beta diversity was calculated using Bray-Curtis, Chao, Jaccard and Unifrac (B). Differentially abundant taxa were identified using LEfSe (C). Dots on each graph in A & B represent individual animals (n = 9–11). LDA: Linear Discriminant Analysis.

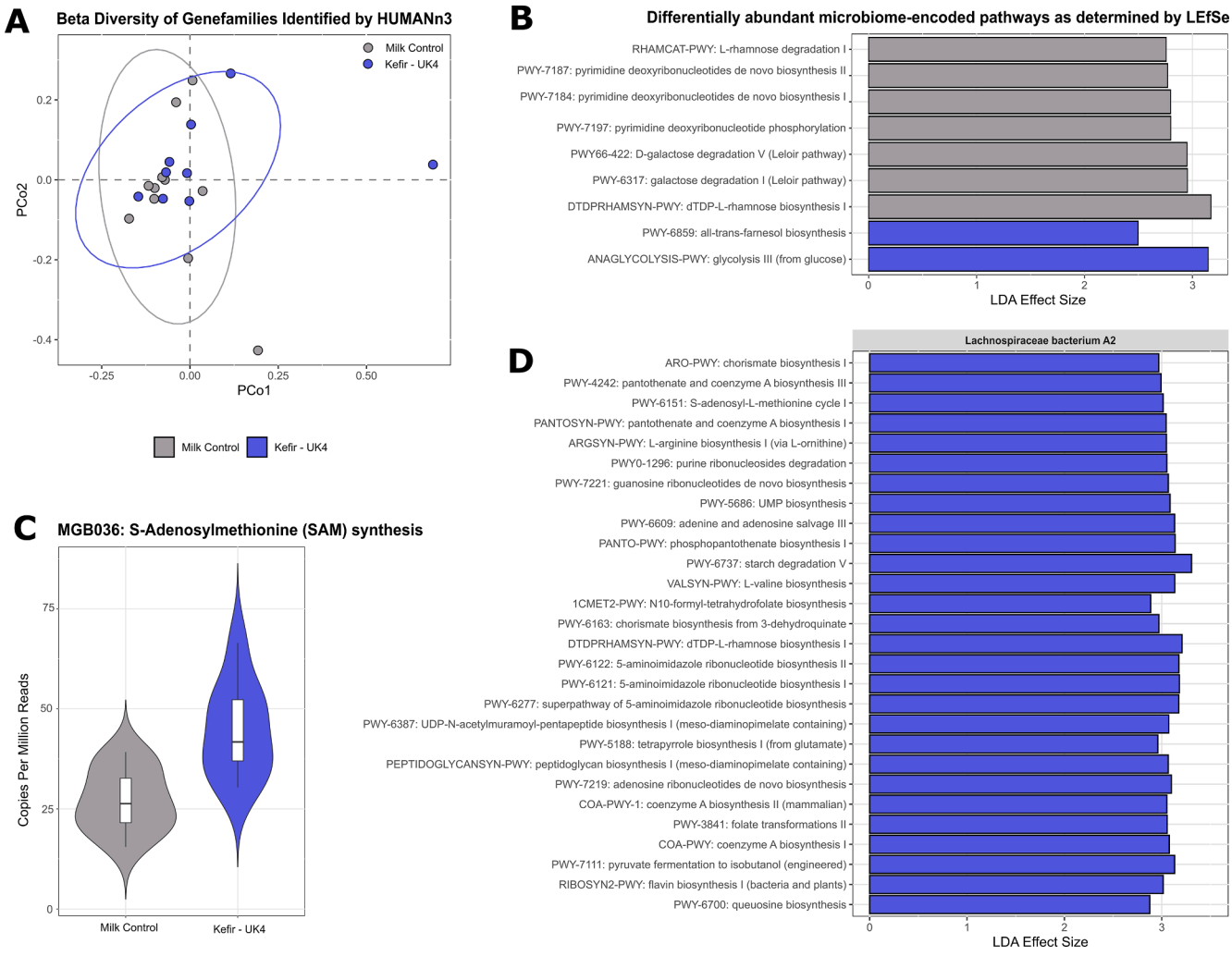

Fig. 7. Kefir modulates selective aspects of the predicted functional microbiome. Beta diversity was calculated based on HUMANn3 UniRef90 gene family abundance profiles (A). Differentially abundant pathways were identified using LEfSe for both the overall microbiome (B) and *Lachnospiraceae bacterium A2* (D). Gut-brain modules (GBMs) were investigated, of which only S-adenosylmethionine (SAM) synthesis was differentially abundant (C). Dots on each graph represent individual animals (n = 9–11). LDA: Linear Discriminant Analysis.

3.12. Lachnospiraceae bacterium A2 correlates with repetitive behaviour and MLN Treg cells following kefir administration

Correlations between gut microbial taxa and behaviour and immunity parameters significantly changed by kefir administration revealed 12 significant correlations (Fig. 8**A**). Importantly, an increased *L. bacterium A2* abundance correlated with reduced marble burying time and increased Treg cells in MLNs (r_s = -0.60, p = 0.007; r_s = 0.49, p = 0.027 respectively) (Fig. 8**B**), which subsequently correlated with marble burying time and Treg cells, where 34 significant correlations were observed (Fig. 8**C**). Importantly, 27 of these pathways (highlighted bold in Fig. 8**C**) were also increased due to the increase in relative *L. bacterium A2* abundance (Fig. 7**D**). Finally, there was a significant correlation between the GBM S-Adenosylmethionine synthesis abundance in *L. bacterium A2* with marble burying time (r_s = -0.67, p = 0.002).

3.13. Key predicted metabolic pathways involved in the effects of kefir UK4 on Treg cells in MLNs and repetitive behaviour

Considering that kefir UK4 reduced repetitive behaviour and increased Treg cells in MLNs in both this study, as well as the previous study (van de Wouw et al., 2020b), we combined both datasets to identify which of the previously identified 27 functional pathways were most likely involved in exerting the effects of kefir. As such, functional pathways were correlated with repetitive behaviour (number of marbles buried) and Treg cells in MLNs using data from both studies (sTable 2). There were 6 functional pathways that associated with Treg cells in MLNs following a correction for multiple comparisons, where 3 were related to glycolysis pathways (PWY66-400: glycolysis VI, $r_s = -0.3135$, q = 0.027; GLYCOLYSIS: glycolysis I, $r_s = -0.2417$, q = 0.036; PWY-5484: glycolysis II, $r_s = -0.2734$, q = 0.036), while the rest were associated with L-histidine degradation (HISDEG-PWY, $r_s = 0.1319$, q = 0.036), L-valine biosynthesis (VALSYN-PWY, $r_s = 0.2099$, q = 0.022), and pyruvate fermentation to isobutanol (PWY-7111, $r_s = 0.2099$, q = 0.022). Notably, both L-valine biosynthesis and pyruvate fermentation to isobutanol pathways were present in *L. bacterium A2* and correlated with marble burying, indicating that these might be key pathways through which kefir UK4 exerts its effects on Treg cells in MLNs and repetitive behaviour.

4. Discussion

In the present study, we demonstrate that kefir supplementation was well-tolerated and improved the repetitive behaviour of BTBR mice, a mouse model of ASD (Golubeva et al., 2017). In addition, kefir

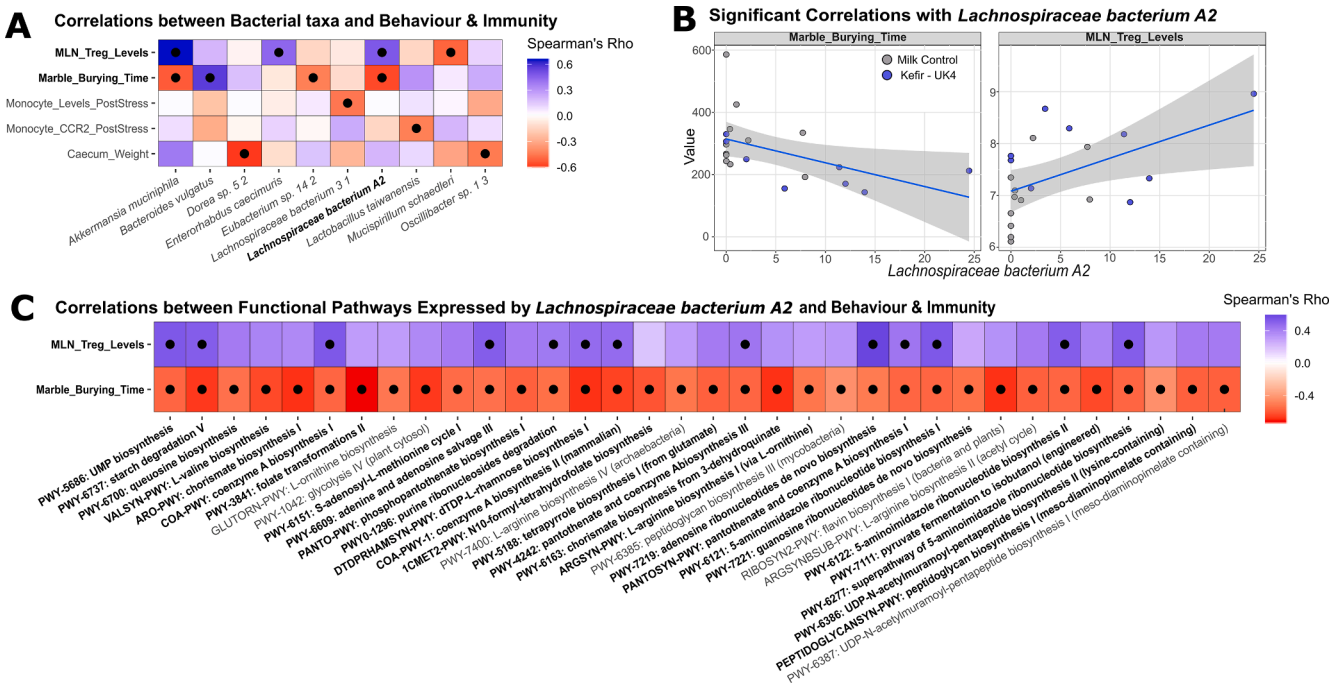

Fig. 8. *Lachnospiraceae bacterium A2* correlates with repetitive behavior and MLN Treg cells. Correlations were performed using HAllA between bacterial taxa with behaviour and immune measurements (A, B). Correlations were subsequently performed between functional pathways and behaviour and immune measurements (C), after which significant pathways were marked bold if they were significantly enriched in mice receiving kefir. Dots on panels A and B represent individual animals (n = 9–11) while dots on panel C represent statistically significant correlations.

prolonged stress-induced corticosterone responses and ameliorated the immune response to an acute stressor. Finally, kefir increased the level of anti-inflammatory Treg cells in MLNs of BTBR mice.

Many of the behavioural and physiological findings are consistent with our previous data in normal C57BL/6 mice (van de Wouw et al., 2020b). For instance, these previous studies showed that kefir UK4 decreased repetitive behaviour and increased Treg cells in MLNs, whereas other measures of anxiety and depressive-like behaviour, gastrointestinal motility and gut serotonin levels remained unaffected in control mice. Some divergence did emerge between the effects of kefir UK4 in BTBR mice versus that shown in C57BL/6 mice, with kefir UK4 failing to increase fear-dependent contextual learning or peripheral Treg cell levels in the former strain. These latter differences might be explained by the way kefir affects these different mouse strains as, for instance, fear-dependent learning is decreased in BTBR mice (Stapley et al., 2013). Overall, this indicates that the physiological and behavioural effects of the fermented milk drink kefir are reproducible.

We show that specific behavioural deficits in BTBR mice, such as an increased engagement in repetitive behaviour (Golubeva et al., 2017), were alleviated. Furthermore, mice receiving kefir showed social recognition, which was absent in mice receiving milk. Nonetheless, no significant difference was found in the social recognition index between the two groups, indicating that more research is warranted to validate if kefir can ameliorate social impairments associated with ASD. Previous studies have also indicated that the gut microbiota provides a potential therapeutic target for ASD (Hsiao et al., 2013; Kumar and Sharma, 2016). For instance, repeated intraperitoneal administration of the gut microbial-derived metabolite butyrate has also been shown to attenuate social deficits and repetitive behaviour in BTBR mice (Kratsman et al., 2016). These observed changes were associated with increased GABAergic signalling in the prefrontal cortex as indicated by increased GABA receptor subunit gamma-1 gene expression. In addition, subsequent administration of a reverse agonist of the $GABA_A$ receptor reversed the effects of butyrate on social deficits, indicating that butyrate ameliorates social deficits in BTBR mice by enhancing GABAergic signalling (Kratsman et al., 2016). Similarly, the consumption of a fermented milk product containing probiotic bacteria changed the activity of the prefrontal cortex in healthy women (Tillisch et al., 2013). We have previously shown that this kefir increases the capacity of the gut microbiota to produce GABA (van de Wouw et al., 2020b), indicating that kefir might have increased GABA signalling in this study.

The BTBR mouse model also displays a persistent immune dysregulation, similar to what has been reported in individuals with ASD (Careaga et al., 2015). For instance, elevated T cell activation in circulation (Ashwood et al., 2011a), decreased anti-inflammatory Treg cells (Ahmad et al., 2017), and increased IFNγ expression and Th1/2 ratio in the cortex have been reported (Li et al., 2009). Similarly, BTBR mice show increased T helper cell activation, decreased levels of anti-inflammatory Treg cells and changes in transcription factor expression associated with T helper cell subsets in the CNS (Zhang et al., 2013; Bakheet et al., 2017). Our data demonstrated that kefir administration increases the prevalence of Treg cells in MLNs, even though Treg cell and IL-10 levels remained unaffected in peripheral circulation.

Our data also showed that kefir prolonged stress-induced increases in plasma corticosterone 60 min post-stress. Even though acute stress, as well as increases in corticosterone, have previously been associated with innate immune cell trafficking and activation (Böbel et al., 2018; Boehme et al., 2020; Dhabhar et al., 2012; van de Wouw et al., 2020a), kefir ameliorated acute stress-induced $LY6C^{hi}$ monocyte decreases, which was associated with a trend towards a reduced stress-induced expression of the trafficking receptor CCR2 (Prinz and Priller 2010). It is therefore interesting to note that stress-induced changes in glucocorticoids have been implicated in both the activation of the immune system and suppression of ongoing stress responses (Sapolsky et al., 2000; van de Wouw et al., 2019). One might postulate that the initial stress-induced increase in corticosterone facilitates immune cell trafficking, after which corticosterone could contribute to the recovery of stress-induced immune cell trafficking. Alternatively, the increased levels of peripheral $LY6C^{hi}$ monocytes may also reflect an increased mobilization of myeloid cells from the bone marrow or spleen (Swirski et al., 2009; Wohleb et al., 2013). Nonetheless, the finding that kefir ameliorated stress-induced decreases in $LY6C^{hi}$ monocyte and CCR2

receptor expression may indicate decreased LY6C^{hi} monocyte trafficking into the CNS (Prinz and Priller 2010). Interestingly, ASD is associated with elevated levels of circulating cytokines associated with the innate immune system, such as IL-1β, IL-6, IL-8 and IL-12 (Ashwood et al., 2011b). In addition, increased levels of IL-1β, IL-6, IL-8 and TNFα have been reported in the cortex of individuals with ASD (Li et al., 2009b), and increased levels of CCL2, IL6, TGF-β1 and IGFBP-1 have been demonstrated in the cerebellum, middle frontal gyrus and anterior cingulate gyrus (Vargas et al., 2005). Furthermore, microglia activation and increased microglia density have been reported in the dorsolateral prefrontal cortex of ASD individuals (Morgan et al., 2010). Similarly, macrophages derived from BTBR mice secrete more inflammatory cytokines, which correlates with their ASD-associated behavioural phenotype (Onore et al., 2013). Overall, these data indicate that kefir may modulate peripheral immunoregulation, which might have relevance to neuroimmune activation (Reader et al., 2015; Kim et al., 2018). Future research should address whether these kefir-induced changes in acute stress-induced LY6C^{hi} monocyte decreases have relevance to neuroinflammation. It is therefore interesting to note that kefir has been shown to reduce microglial activation in spontaneously hypertensive rats (de Almeida Silva et al., 2020).

In line with previous work (van de Wouw et al., 2020b), kefir did not impact gut 5-HT levels and gastrointestinal motility, even though kefir did increase cecum weight. Interestingly, germ-free mice, as well as mice receiving the prebiotic GOS/inulin or antibiotics have been shown to have increased caecum sizes (Barrat et al., 2008; Grover and Kashyap, 2014; Kang et al., 2017b), indicating that an altered cecum weight is neither good nor bad *per se*. Finally, no differences in ileal or colonic permeability were observed. In line with these findings is an absence of change in colonic mucosal layer thickness, which represents an additional barrier against the infiltration of gut microbes and their products into the host circulation (Johansson et al., 2011).

Analysis of the caecal microbiome revealed no changes in alpha and beta diversity following kefir administration, which is in line with a previous study from our lab in C57BL/6j mice (van de Wouw et al., 2020b). Kefir did increase relative *L. bacterium A2* abundance and reduced the relative abundance of the *Clostridium* genus and *Clostridiaceae*, the latter being a pattern that has been reported previously in mice (Marquina et al., 2002). Interestingly, the relative abundance of the *Lachnospiraceae* family is reduced in BTBR mice (Golubeva et al., 2017), and in humans with ASD in some (Cao et al., 2021), but not all (Zhang et al., 2021), reports. Notably, although gut microbial changes in ASD patients are well-documented, specific microbial signature for the ASD autistic gut has been elusive (Fattorusso et al., 2019; Andreo-Martínez et al., 2020). *L. bacterium A2* and its functional potential also correlated with repetitive behaviour and Treg cells in MLNs and, although correlation does not necessarilly imply causation, it will be intriguing to further investigate a potential role for this taxon in kefir-induced effects on behaviour and immunity in this mouse strain. Importantly, *L. bacterium A2* is not a member of the kefir microbiota and was detected in only 1 mouse in the previous study with C57BL/6 mice, with no increase in *L. bacterium A2* being observed in that instance (data not shown), despite a decrease in repetitive behaviour and MLN Treg cells being observed in that study (van de Wouw et al., 2020b). Differences in host genetics or baseline microbiome may contribute to differences across the two murine models.

It was notable from a microbiome perspective that kefir increased the relative abundance of the GBM SAM, which was also previously reported in C57BL/6j mice (van de Wouw et al., 2020b). Decreased SAM levels have been reported in individuals with ASD (James et al., 2004), while both increased and decreased methionine levels have been reported (Zheng et al., 2017). It is interesting to note that oral administration of SAM ameliorates repetitive behaviour and gene expression in the prefrontal cortex in a different valproic acid-induced ASD model in male mice (Ornoy et al., 2019; Weinstein-Fudim et al., 2019). Further analysis of the predicted function of the gut microbiome and its association with repetitive behaviour and Treg cells in MLNs using this study and a previously published kefir study revealed that L-valine biosynthesis and pyruvate fermentation to isobutanol pathways may mediate these kefir UK4-induced effects. Notably, some other studies have reported elevated levels of valine and pyruvate in individuals with ASD (Legido et al., 2013; Zou et al., 2020).

Finally, given that ASD is a neurodevelopmental disorder (Lyall et al., 2017) and the supplementation of kefir in the present study started in adulthood, it may be that starting kefir administration at an earlier stage of life could lead to an even greater amelioration of some of the other physiological or behavioural deficits present in BTBR mice, which remained unaffected in this study. Furthermore, different kefirs have been demonstrated to impact the gut microbiome, host immunity, behaviour and metabolism in distinct ways (Bourrie et al., 2021; van de Wouw et al., 2020b). As such, the observed effects of the kefir strain in this study might not translate to other kefir beverages or, indeed, beverages may exist that have even more profound impacts.

5. Conclusions

These data demonstrate that the traditionally fermented milk drink kefir reduces specific behavioural impairments, as well as modulate peripheral immunoregulation, in a mouse model of ASD. These results reinforce the notion of kefir as a potential intervention to positively modulate the microbiota-gut-brain axis and show that kefir supplementation might prove a viable strategy in improving specific symptoms in ASD. Moreover, it further confirms the potential of microbiota targeted nutritional interventions that may support mental health (Berding et al., 2021). Finally, studies on the validation of kefir as a dietary intervention to improve ASD symptomatology in a clinical setting are now warranted.

Acknowledgements

Flow cytometry analysis was performed at the APC Microbiome Ireland Flow Cytometry Platform located at University College Cork. The authors are also grateful for the technical assistance of P. Fitzgerald and C. Manley, and the assistance with data analysis and study design by Drs G. Moloney, A. Golubeva and K. J. O'Riordan.

Availability of data and material

Raw microbiota reads have been deposited to the European Nucleotide Archive under the project accession number PRJEB44042.

Funding Sources and Declaration of Interests

The APC Microbiome Ireland is a research institute funded by Science Foundation Ireland (SFI) through the Irish Government's National Development Plan. J.F.C, T.G.D and P.D.C. are supported by SFI (Grant No. SFI/12/RC/2273_P2). MB is supported by an educational grant from Science Foundation Ireland (SFI), Ireland (No. 15/JP-HDHL/3270; JPI-HDHL-NutriCog project 'AMBROSIAC'). J.F.C and T.G.D have research support from Mead Johnson, Cremo, 4D Pharma, Dupont, and Nutricia. P.D.C has research support from PepsiCo, PrecisionBiotics Group and Danone. J.F.C, T.G.D and P.D.C. have spoken at meetings sponsored by food and pharmaceutical companies. All other authors report no potential conflicts of interest.

Appendix A. Supplementary data

Supplementary data to this article can be found online at https://doi.org/10.1016/j.bbi.2021.07.004.

References

Ahmad, S.F., Zoheir, K.M.A., Ansari, M.A., Nadeem, A., Bakheet, S.A., AL-Ayadhi, L.Y., Alzahrani, M.Z., Al-Shabanah, O.A., Al-Harbi, M.M., Attia, S.M., 2017. Dysregulation of Th1, Th2, Th17, and T regulatory cell-related transcription factor signaling in children with autism. Mol Neurobiol 54 (6), 4390–4400.

Andreo-Martínez, P., García-Martínez, N., Sánchez-Samper, E.P., Martínez-González, A. E., 2020. An approach to gut microbiota profile in children with autism spectrum disorder. Environ Microbiol Rep 12 (2), 115–135.

Andrews, S. (2010). FASTQC. A quality control tool for high throughput sequence data.

Ashwood, P., Corbett, B.A., Kantor, A., Schulman, H., Van de Water, J., Amaral, D.G., 2011a. In search of cellular immunophenotypes in the blood of children with autism. PLoS ONE 6 (5), e19299.

Ashwood, P., Krakowiak, P., Hertz-Picciotto, I., Hansen, R., Pessah, I., Van de Water, J., 2011b. Elevated plasma cytokines in autism spectrum disorders provide evidence of immune dysfunction and are associated with impaired behavioral outcome. Brain Behav Immun 25 (1), 40–45.

Aslam, H., Green, J., Jacka, F.N., Collier, F., Berk, M., Pasco, J., Dawson, S.L., 2020. Fermented foods, the gut and mental health: a mechanistic overview with implications for depression and anxiety. Nutr Neurosci 23 (9), 659–671.

Asnicar, F., Thomas, A.M., Beghini, F., Mengoni, C., Manara, S., Manghi, P., Zhu, Q., Bolzan, M., Cumbo, F., May, U., Sanders, J.G., Zolfo, M., Kopylova, E., Pasolli, E., Knight, R., Mirarab, S., Huttenhower, C., Segata, N., 2020. Precise phylogenetic analysis of microbial isolates and genomes from metagenomes using PhyloPhlAn 3.0. Nat Commun 11 (1), 2500.

Association, A. P. (2013). "Diagnostic and Statistical Manual of Mental Disorders (DSM-5®).".

Bakheet, S.A., Alzahrani, M.Z., Ansari, M.A., Nadeem, A., Zoheir, K.M.A., Attia, S.M., Al-Ayadhi, L.Y., Ahmad, S.F., 2017. Resveratrol Ameliorates Dysregulation of Th1, Th2, Th17, and T Regulatory Cell-Related Transcription Factor Signaling in a BTBR T + tf/J Mouse Model of Autism. Mol Neurobiol 54 (7), 5201–5212.

Barrat, E., Michel, C., Poupeau, G., David-Sochard, A., Rival, M., Pagniez, A., Champ, M., Darmaun, D., 2008. Supplementation with galactooligosaccharides and inulin increases bacterial translocation in artificially reared newborn rats. Pediatr Res 64 (1), 34–39.

Beghini, F., L. J. McIver, A. Blanco-Míguez, L. Dubois, F. Asnicar, S. Maharjan, A. Mailyan, A. M. Thomas, P. Manghi, M. Valles-Colomer, G. Weingart, Y. Zhang, M. Zolfo, C. Huttenhower, E. A. Franzosa and N. Segata (2020). "Integrating taxonomic, functional, and strain-level profiling of diverse microbial communities with bioBakery 3." bioRxiv: 2020.2011.2019.388223.

Berding, K., Vlckova, K., Marx, W., Schellekens, H., Stanton, C., Clarke, G., Jacka, F., Dinan, T.G., Cryan, J.F., 2021. "Diet and the Microbiota-Gut-Brain Axis: Sowing the Seeds of Good Mental Health." Adv Nutr 2021 Mar 9;nmaa181.

Blasche, S., Kim, Y., Mars, R.A.T., Machado, D., Maansson, M., Kafkia, E., Milanese, A., Zeller, G., Teusink, B., Nielsen, J., Benes, V., Neves, R., Sauer, U., Patil, K.R., 2021. Metabolic cooperation and spatiotemporal niche partitioning in a kefir microbial community. Nat Microbiol 6 (2), 196–208.

Böbel, T.S., Hackl, S.B., Langgartner, D., Jarczok, M.N., Rohleder, N., Rook, G.A., Lowry, C.A., Gündel, H., Waller, C., Reber, S.O., 2018. Less immune activation following social stress in rural vs. urban participants raised with regular or no animal contact, respectively. Proc Natl Acad Sci U S A 115 (20), 5259–5264.

Boehme, M., K. E. Guzzetta, T. F. S. Bastiaanssen, M. Van de Wouw, G. M. Moloney, A. Gual-Grua, S. Spichak, L. Olavarria-Ramirez, P. Fitzgerald, E. Morillas, N. L. Ritz, M. Jaggar, C. S. M. Cowan, F. Crispie, F. Donoso, E. Halitzki, M. C. Neto, M. Sichetti, A. V. Golubeva, R. S. Fitzgerald, M. J. Claesson, P. D. Cotter, O. F. O'Leary, T. G. Dinan and J. F. Cryan (2021). "Microbiota from Young Mice Counteracts Selective Age-Associated Behavioral Deficits." Nature Aging In press.

Boehme, M., van de Wouw, M., Bastiaanssen, T.F.S., Olavarría-Ramírez, L., Lyons, K., Fouhy, F., Golubeva, A.V., Moloney, G.M., Minuto, C., Sandhu, K.V., Scott, K.A., Clarke, G., Stanton, C., Dinan, T.G., Schellekens, H., Cryan, J.F., 2020. Mid-life microbiota crises: middle age is associated with pervasive neuroimmune alterations that are reversed by targeting the gut microbiome. Mol Psychiatry 25 (10), 2567–2583.

Bourrie, B.C., Willing, B.P., Cotter, P.D., 2016. The Microbiota and Health Promoting Characteristics of the Fermented Beverage Kefir. Front Microbiol 7, 647.

Bourrie, B.C.T., Ju, T., Fouhse, J.M., Forgie, A.J., Sergi, C., Cotter, P.D., Willing, B.P., 2021. Kefir microbial composition is a deciding factor in the physiological impact of kefir in a mouse model of obesity. Br J Nutr 125 (2), 129–138.

Burokas, A., Arboleya, S., Moloney, R.D., Peterson, V.L., Murphy, K., Clarke, G., Stanton, C., Dinan, T.G., Cryan, J.F., 2017. Targeting the Microbiota-Gut-Brain Axis: Prebiotics Have Anxiolytic and Antidepressant-like Effects and Reverse the Impact of Chronic Stress in Mice. Biol Psychiatry 82 (7), 472–487.

Cao, X., Liu, K., Liu, J., Liu, Y.W., Xu, L., Wang, H., Zhu, Y., Wang, P., Li, Z., Wen, J., Shen, C., Li, M., Nie, Z., Kong, X.J., 2021. Dysbiotic Gut Microbiota and Dysregulation of Cytokine Profile in Children and Teens With Autism Spectrum Disorder. Front Neurosci 15, 635925.

Careaga, M., Schwartzer, J., Ashwood, P., 2015. Inflammatory profiles in the BTBR mouse: how relevant are they to autism spectrum disorders? Brain Behav Immun 43, 11–16.

Chen, H.-L., Lan, Y.-W., Tu, M.-Y., Tung, Y.-T., Chan, M.-Y., Wu, H.-S., Yen, C.-C., Chen, C.-M., 2021. Kefir peptides exhibit antidepressant-like activity in mice through the BDNF/TrkB pathway. J Dairy Sci 104 (6), 6415–6430.

Chen, J., Bittinger, K., Charlson, E.S., Hoffmann, C., Lewis, J., Wu, G.D., Collman, R.G., Bushman, F.D., Li, H., 2012. Associating microbiome composition with environmental covariates using generalized UniFrac distances. Bioinformatics 28 (16), 2106–2113.

Clarke, G., Grenham, S., Scully, P., Fitzgerald, P., Moloney, R.D., Shanahan, F., Dinan, T. G., Cryan, J.F., 2013. The microbiome-gut-brain axis during early life regulates the hippocampal serotonergic system in a sex-dependent manner. Mol Psychiatry 18 (6), 666–673.

Collins, S.M., Surette, M., Bercik, P., 2012. The interplay between the intestinal microbiota and the brain. Nat Rev Microbiol 10 (11), 735–742.

Coretti, L., Cristiano, C., Florio, E., Scala, G., Lama, A., Keller, S., Cuomo, M., Russo, R., Pero, R., Paciello, O., Mattace Raso, G., Meli, R., Cocozza, S., Calignano, A., Chiariotti, L., Lembo, F., 2017. Sex-related alterations of gut microbiota composition in the BTBR mouse model of autism spectrum disorder. Sci Rep 7, 45356.

Cryan, J.F., Dinan, T.G., 2012. Mind-altering microorganisms: the impact of the gut microbiota on brain and behaviour. Nat Rev Neurosci 13 (10), 701–712.

Cryan, J.F., Mombereau, C., 2004. In search of a depressed mouse: utility of models for studying depression-related behavior in genetically modified mice. Mol Psychiatry 9 (4), 326–357.

Cryan, J.F., O'Riordan, K.J., Cowan, C.S.M., Sandhu, K.V., Bastiaanssen, T.F.S., Boehme, M., Codagnone, M.G., Cussotto, S., Fulling, C., Golubeva, A.V., Guzzetta, K. E., Jaggar, M., Long-Smith, C.M., Lyte, J.M., Martin, J.A., Molinero-Perez, A., Moloney, G., Morelli, E., Morillas, E., O'Connor, R., Cruz-Pereira, J.S., Peterson, V.L., Rea, K., Ritz, N.L., Sherwin, E., Spichak, S., Teichman, E.M., van de Wouw, M., Ventura-Silva, A.P., Wallace-Fitzsimons, S.E., Hyland, N., Clarke, G., Dinan, T.G., 2019. The Microbiota-Gut-Brain Axis. Physiol Rev 99 (4), 1877–2013.

D'Eufemia, P., Celli, M., Finocchiaro, R., Pacifico, L., Viozzi, L., Zaccagnini, M., Cardi, E., Giardini, O., 1996. Abnormal intestinal permeability in children with autism. Acta Paediatr 85 (9), 1076–1079.

Darzi, Y., Falony, G., Vieira-Silva, S., Raes, J., 2016. Towards biome-specific analysis of meta-omics data. ISME J 10 (5), 1025–1028.

David, M. M. (2021). "The Role of the Microbiome in Autism: All That We Know about All That We Don't Know." mSystems 6(2).

David, M. M., C. Tataru, J. Daniels, J. Schwartz, J. Keating, J. Hampton-Marcell, N. Gottel, J. A. Gilbert and D. P. Wall (2021). "Children with Autism and Their Typically Developing Siblings Differ in Amplicon Sequence Variants and Predicted Functions of Stool-Associated Microbes." mSystems 6(2).

de Almeida Silva, M., Mowry, F.E., Peaden, S.C., Andrade, T.U., Biancardi, V.C., 2020. Kefir ameliorates hypertension via gut-brain mechanisms in spontaneously hypertensive rats. J Nutr Biochem 77, 108318.

De Angelis, M., Piccolo, M., Vannini, L., Siragusa, S., De Giacomo, A., Serrazzanetti, D.I., Cristofori, F., Guerzoni, M.E., Gobbetti, M., Francavilla, R., 2013. Fecal microbiota and metabolome of children with autism and pervasive developmental disorder not otherwise specified. PLoS ONE 8 (10), e76993.

Desbonnet, L., Clarke, G., Shanahan, F., Dinan, T.G., Cryan, J.F., 2014. Microbiota is essential for social development in the mouse. Mol Psychiatry 19 (2), 146–148.

Dhabhar, F.S., Malarkey, W.B., Neri, E., McEwen, B.S., 2012. Stress-induced redistribution of immune cells–from barracks to boulevards to battlefields: a tale of three hormones–Curt Richter Award winner. Psychoneuroendocrinology 37 (9), 1345–1368.

Dobson, A., O'Sullivan, O., Cotter, P.D., Ross, P., Hill, C., 2011. High-throughput sequence-based analysis of the bacterial composition of kefir and an associated kefir grain. FEMS Microbiol Lett 320 (1), 56–62.

Fattorusso, A., Di Genova, L., Dell'Isola, G., Mencaroni, E., Esposito, S., 2019. Autism Spectrum Disorders and the Gut Microbiota. Nutrients 11 (3), 521. https://doi.org/10.3390/nu11030521.

Foster, J.A., Rinaman, L., Cryan, J.F., 2017. Stress & the gut-brain axis: Regulation by the microbiome. Neurobiol Stress 7, 124–136.

Fouquier, J., N. Moreno Huizar, J. Donnelly, C. Glickman, D. W. Kang, J. Maldonado, R. A. Jones, K. Johnson, J. B. Adams, R. Krajmalnik-Brown and C. Lozupone (2021). "The Gut Microbiome in Autism: Study-Site Effects and Longitudinal Analysis of Behavior Change." mSystems 6(2).

Golubeva, A.V., Joyce, S.A., Moloney, G., Burokas, A., Sherwin, E., Arboleya, S., Flynn, I., Khochanskiy, D., Moya-Perez, A., Peterson, V., Rea, K., Murphy, K., Makarova, O., Buravkov, S., Hyland, N.P., Stanton, C., Clarke, G., Gahan, C.G.M., Dinan, T.G., Cryan, J.F., 2017. Microbiota-related Changes in Bile Acid & Tryptophan Metabolism are Associated with Gastrointestinal Dysfunction in a Mouse Model of Autism. EBioMedicine 24, 166–178.

Grover, M., Kashyap, P.C., 2014. Germ-free mice as a model to study effect of gut microbiota on host physiology. Neurogastroenterol Motil 26 (6), 745–748.

Gururajan, A., van de Wouw, M., Boehme, M., Becker, T., O'Connor, R., Bastiaanssen, T. F.S., Moloney, G.M., Lyte, J.M., Ventura Silva, A.P., Merckx, B., Dinan, T.G., Cryan, J.F., 2019. Resilience to chronic stress is associated with specific neurobiological, neuroendocrine and immune responses. Brain Behav Immun 80, 583–594.

Hsiao, E., McBride, S., Hsien, S., Sharon, G., Hyde, E., McCue, T., Codelli, J., Chow, J., Reisman, S., Petrosino, J., Patterson, P., Mazmanian, S., 2013. Microbiota modulate behavioral and physiological abnormalities associated with neurodevelopmental disorders. Cell 155 (7), 1451–1463.

Huerta-Cepas, J., Forslund, K., Coelho, L.P., Szklarczyk, D., Jensen, L.J., von Mering, C., Bork, P., 2017. Fast Genome-Wide Functional Annotation through Orthology Assignment by eggNOG-Mapper. Mol Biol Evol 34 (8), 2115–2122.

Huerta-Cepas, J., Szklarczyk, D., Heller, D., Hernandez-Plaza, A., Forslund, S.K., Cook, H., Mende, D.R., Letunic, I., Rattei, T., Jensen, L.J., von Mering, C., Bork, P., 2019. eggNOG 5.0: a hierarchical, functionally and phylogenetically annotated orthology resource based on 5090 organisms and 2502 viruses. Nucleic Acids Res 47 (D1), D309–D314.

Izquierdo, A., Wellman, C.L., Holmes, A., 2006. Brief uncontrollable stress causes dendritic retraction in infralimbic cortex and resistance to fear extinction in mice. J Neurosci 26 (21), 5733–5738.

James, S.J., Cutler, P., Melnyk, S., Jernigan, S., Janak, L., Gaylor, D.W., Neubrander, J. A., 2004. Metabolic biomarkers of increased oxidative stress and impaired methylation capacity in children with autism. Am J Clin Nutr 80 (6), 1611–1617.

Johansson, M.E.V., Ambort, D., Pelaseyed, T., Schütte, A., Gustafsson, J.K., Ermund, A., Subramani, D.B., Holmén-Larsson, J.M., Thomsson, K.A., Bergström, J.H., van der Post, S., Rodriguez-Piñeiro, A.M., Sjövall, H., Bäckström, M., Hansson, G.C., 2011. Composition and functional role of the mucus layers in the intestine. Cell Mol Life Sci 68 (22), 3635–3641.

Kang, D.D., Li, F., Kirton, E., Thomas, A., Egan, R., An, H., Wang, Z., 2019a. MetaBAT 2: an adaptive binning algorithm for robust and efficient genome reconstruction from metagenome assemblies. PeerJ 7, e7359.

Kang, D.W., Adams, J.B., Coleman, D.M., Pollard, E.L., Maldonado, J., McDonough-Means, S., Caporaso, J.G., Krajmalnik-Brown, R., 2019b. Long-term benefit of Microbiota Transfer Therapy on autism symptoms and gut microbiota. Sci Rep 9 (1), 5821.

Kang, D.W., Adams, J.B., Gregory, A.C., Borody, T., Chittick, L., Fasano, A., Khoruts, A., Geis, E., Maldonado, J., McDonough-Means, S., Pollard, E.L., Roux, S., Sadowsky, M. J., Lipson, K.S., Sullivan, M.B., Caporaso, J.G., Krajmalnik-Brown, R., 2017a. Microbiota Transfer Therapy alters gut ecosystem and improves gastrointestinal and autism symptoms: an open-label study. Microbiome 5 (1), 10.

Kang, D.W., Park, J.G., Ilhan, Z.E., Wallstrom, G., Labaer, J., Adams, J.B., Krajmalnik-Brown, R., 2013. Reduced incidence of Prevotella and other fermenters in intestinal microflora of autistic children. PLoS ONE 8 (7), e68322.

Kang, M., Mischel, R.A., Bhave, S., Komla, E., Cho, A., Huang, C., Dewey, W.L., Akbarali, H.I., 2017b. The effect of gut microbiome on tolerance to morphine mediated antinociception in mice. Sci Rep 7, 42658.

Kembel, S.W., Cowan, P.D., Helmus, M.R., Cornwell, W.K., Morlon, H., Ackerly, D.D., Blomberg, S.P., Webb, C.O., 2010. Picante: R tools for integrating phylogenies and ecology. Bioinformatics 26 (11), 1463–1464.

Kim, J.W., Hong, J.Y., Bae, S.M., 2018. Microglia and Autism Spectrum Disorder: Overview of Current Evidence and Novel Immunomodulatory Treatment Options. Clin Psychopharmacol Neurosci 16 (3), 246–252.

Kratsman, N., Getselter, D., Elliott, E., 2016. Sodium butyrate attenuates social behavior deficits and modifies the transcription of inhibitory/excitatory genes in the frontal cortex of an autism model. Neuropharmacology 102, 136–145.

Kumar, H., Sharma, B., 2016. Minocycline ameliorates prenatal valproic acid induced autistic behaviour, biochemistry and blood brain barrier impairments in rats. Brain Res 1630, 83–97.

Langgartner, D., Lowry, C.A., Reber, S.O., 2019. Old Friends, immunoregulation, and stress resilience. Pflugers Arch 471 (2), 237–269.

Langmead, B., Salzberg, S.L., 2012. Fast gapped-read alignment with Bowtie 2. Nat Methods 9 (4), 357–359.

Legido, A., Jethva, R., Goldenthal, M.J., 2013. Mitochondrial dysfunction in autism. Semin Pediatr Neurol 20 (3), 163–175.

Li, H., Handsaker, B., Wysoker, A., Fennell, T., Ruan, J., Homer, N., Marth, G., Abecasis, G., Durbin, R., 2009a. The Sequence Alignment/Map format and SAMtools. Bioinformatics 25 (16), 2078–2079.

Li, X., Chauhan, A., Sheikh, A.M., Patil, S., Chauhan, V., Li, X.M., Ji, L., Brown, T., Malik, M., 2009b. Elevated immune response in the brain of autistic patients. J Neuroimmunol 207 (1–2), 111–116.

Lowry, C.A., Smith, D.G., Siebler, P.H., Schmidt, D., Stamper, C.E., Hassell, J.E., Yamashita, P.S., Fox, J.H., Reber, S.O., Brenner, L.A., Hoisington, A.J., Postolache, T. T., Kinney, K.A., Marciani, D., Hernandez, M., Hemmings, S.M.J., Malan-Muller, S., Wright, K.P., Knight, R., Raison, C.L., Rook, G.A.W., 2016. The Microbiota, Immunoregulation, and Mental Health: Implications for Public Health. Curr Environ Health Rep 3 (3), 270–286.

Luna, R.A., Oezguen, N., Balderas, M., Venkatachalam, A., Runge, J.K., Versalovic, J., Veenstra-VanderWeele, J., Anderson, G.M., Savidge, T., Williams, K.C., 2017. Distinct Microbiome-Neuroimmune Signatures Correlate With Functional Abdominal Pain in Children With Autism Spectrum Disorder. Cell Mol Gastroenterol Hepatol 3 (2), 218–230.

Lyall, K., Croen, L., Daniels, J., Fallin, M.D., Ladd-Acosta, C., Lee, B.K., Park, B.Y., Snyder, N.W., Schendel, D., Volk, H., Windham, G.C., Newschaffer, C., 2017. The Changing Epidemiology of Autism Spectrum Disorders. Annu Rev Public Health 38, 81–102.

Marquina, D., Santos, A., Corpas, I., Munoz, J., Zazo, J., Peinado, J.M., 2002. Dietary influence of kefir on microbial activities in the mouse bowel. Lett Appl Microbiol 35 (2), 136–140.

Martin, M., 2011. Cutadapt removes adapter sequences from high-throughput sequencing reads. EMBnet.journal 17 (1), 10.

Mayer, E.A., Knight, R., Mazmanian, S.K., Cryan, J.F., Tillisch, K., 2014. Gut Microbes and the Brain: Paradigm Shift in Neuroscience. The Journal of Neuroscience 34 (46), 15490.

McElhanon, B.O., McCracken, C., Karpen, S., Sharp, W.G., 2014. Gastrointestinal symptoms in autism spectrum disorder: a meta-analysis. Pediatrics 133 (5), 872–883.

Morgan, J.T., Chana, G., Pardo, C.A., Achim, C., Semendeferi, K., Buckwalter, J., Courchesne, E., Everall, I.P., 2010. Microglial activation and increased microglial density observed in the dorsolateral prefrontal cortex in autism. Biol Psychiatry 68 (4), 368–376.

Moy, S.S., Nadler, J.J., Young, N.B., Perez, A., Holloway, L.P., Barbaro, R.P., Barbaro, J. R., Wilson, L.M., Threadgill, D.W., Lauder, J.M., Magnuson, T.R., Crawley, J.N., 2007. Mouse behavioral tasks relevant to autism: phenotypes of 10 inbred strains. Behav Brain Res 176 (1), 4–20.

Murray, E., Sharma, R., Smith, K.B., Mar, K.D., Barve, R., Lukasik, M., Pirwani, A.F., Malette-Guyon, E., Lamba, S., Thomas, B.J., Sadeghi-Emamchaie, H., Liang, J., Mallet, J.F., Matar, C., Ismail, N., 2019. Probiotic consumption during puberty mitigates LPS-induced immune responses and protects against stress-induced depression- and anxiety-like behaviors in adulthood in a sex-specific manner. Brain Behav Immun 81, 198–212.

Nurk, S., Meleshko, D., Korobeynikov, A., Pevzner, P.A., 2017. metaSPAdes: a new versatile metagenomic assembler. Genome Res 27 (5), 824–834.

O'Connor, R., van De Wouw, M., Moloney, G.M., Ventura-Silva, A.P., O'Riordan, K., Golubeva, A.V., Dinan, T.G., Schellekens, H., Cryan, J.F., 2021. Strain differences in behaviour and immunity in aged mice: Relevance to Autism. Behav Brain Res 399, 113020.

Oksanen, J., F. G. Blanchet, M. Friendly, R. Kindt, P. Legendre, D. McGlinn, P. R. Minchin, R. B. O'Hara, G. L. Simpson, P. Solymos, M. H. H. Stevens, E. Szoecs and H. Wagner (2020). vegan: Community Ecology Package.

Onore, C.E., Careaga, M., Babineau, B.A., Schwartzer, J.J., Berman, R.F., Ashwood, P., 2013. Inflammatory macrophage phenotype in BTBR T+tf/J mice. Front Neurosci 7, 158.

Ornoy, A., Weinstein-Fudim, L., Tfilin, M., Ergaz, Z., Yanai, J., Szyf, M., Turgeman, G., 2019. S-adenosyl methionine prevents ASD like behaviors triggered by early postnatal valproic acid exposure in very young mice. Neurotoxicol Teratol 71, 64–74.

Parks, D.H., Imelfort, M., Skennerton, C.T., Hugenholtz, P., Tyson, G.W., 2015. CheckM: assessing the quality of microbial genomes recovered from isolates, single cells, and metagenomes. Genome Res 25 (7), 1043–1055.

Prinz, M., Priller, J., 2010. Tickets to the brain: role of CCR2 and CX3CR1 in myeloid cell entry in the CNS. J Neuroimmunol 224 (1–2), 80–84.

Quinlan, A.R., Hall, I.M., 2010. BEDTools: a flexible suite of utilities for comparing genomic features. Bioinformatics 26 (6), 841–842.

Rahnavard, G., E. A. Franzosa, L. J. McIver, E. Schwager, J. Lloyd-Price, G. Weingart, Y. S. Moon, X. C. Morgan, L. Waldron and C. Huttenhower. "High-sensitivity pattern discovery in large multi'omic datasets." from https://github.com/biobakery/halla.

Reader, B.F., Jarrett, B.L., McKim, D.B., Wohleb, E.S., Godbout, J.P., Sheridan, J.F., 2015. Peripheral and central effects of repeated social defeat stress: monocyte trafficking, microglial activation, and anxiety. Neuroscience 289, 429–442.

Rhee, S.H., Pothoulakis, C., Mayer, E.A., 2009. Principles and clinical implications of the brain-gut-enteric microbiota axis. Nat Rev Gastroenterol Hepatol 6 (5), 306–314.

Sabat, R., Grütz, G., Warszawska, K., Kirsch, S., Witte, E., Wolk, K., Geginat, J., 2010. Biology of interleukin-10. Cytokine Growth Factor Rev 21 (5), 331–344.

Sapolsky, R.M., Romero, L.M., Munck, A.U., 2000. How do glucocorticoids influence stress responses? Integrating permissive, suppressive, stimulatory, and preparative actions. Endocr Rev 21 (1), 55–89.

Seemann, T., 2014. Prokka: rapid prokaryotic genome annotation. Bioinformatics 30 (14), 2068–2069.

Segata, N., Izard, J., Waldron, L., Gevers, D., Miropolsky, L., Garrett, W.S., Huttenhower, C., 2011. Metagenomic biomarker discovery and explanation. Genome Biol 12 (6), R60.

Sgritta, M., Dooling, S.W., Buffington, S.A., Momin, E.N., Francis, M.B., Britton, R.A., Costa-Mattioli, M., 2019. Mechanisms Underlying Microbial-Mediated Changes in Social Behavior in Mouse Models of Autism Spectrum Disorder. Neuron 101 (2), 246–259 e246.

Sharon, G., Cruz, N.J., Kang, D.W., Gandal, M.J., Wang, B., Kim, Y.M., Zink, E.M., Casey, C.P., Taylor, B.C., Lane, C.J., Bramer, L.M., Isern, N.G., Hoyt, D.W., Noecker, C., Sweredoski, M.J., Moradian, A., Borenstein, E., Jansson, J.K., Knight, R., Metz, T.O., Lois, C., Geschwind, D.H., Krajmalnik-Brown, R., Mazmanian, S.K., 2019. Human Gut Microbiota from Autism Spectrum Disorder Promote Behavioral Symptoms in Mice. Cell 177 (6), 1600–1618 e1617.

Sherwin, E., Bordenstein, S.R., Quinn, J.L., Dinan, T.G., Cryan, J.F., 2019. Microbiota and the social brain. Science 366 (6465), eaar2016. https://doi.org/10.1126/science:aar2016.

Stapley, N.W., Guariglia, S.R., Chadman, K.K., 2013. Cued and contextual fear conditioning in BTBR mice is improved with training or atomoxetine. Neurosci Lett 549, 120–124.

Swirski, F.K., Nahrendorf, M., Etzrodt, M., Wildgruber, M., Cortez-Retamozo, V., Panizzi, P., Figueiredo, J.-L., Kohler, R.H., Chudnovskiy, A., Waterman, P., Aikawa, E., Mempel, T.R., Libby, P., Weissleder, R., Pittet, M.J., 2009. Identification of splenic reservoir monocytes and their deployment to inflammatory sites. Science 325 (5940), 612–616.

Tillisch, K., J. Labus, L. Kilpatrick, Z. Jiang, J. Stains, B. Ebrat, D. Guyonnet, S. Legrain–Raspaud, B. Trotin and B. Naliboff (2013). "Consumption of fermented milk product with probiotic modulates brain activity." Gastroenterology 144(7): 1394-1401. e1394.

Tomova, A., Husarova, V., Lakatosova, S., Bakos, J., Vlkova, B., Babinska, K., Ostatnikova, D., 2015. Gastrointestinal microbiota in children with autism in Slovakia. Physiol Behav 138, 179–187.

Valles-Colomer, M., Falony, G., Darzi, Y., Tigchelaar, E.F., Wang, J., Tito, R.Y., Schiweck, C., Kurilshikov, A., Joossens, M., Wijmenga, C., Claes, S., Van Oudenhove, L., Zhernakova, A., Vieira-Silva, S., Raes, J., 2019. The neuroactive potential of the human gut microbiota in quality of life and depression. Nat Microbiol 4 (4), 623–632.

van de Wouw, M., Boehme, M., Dinan, T.G., Cryan, J.F., 2019. Monocyte mobilisation, microbiota & mental illness. Brain Behav Immun 81, 74–91.

van de Wouw, M., Boehme, M., Lyte, J.M., Wiley, N., Strain, C., O'Sullivan, O., Clarke, G., Stanton, C., Dinan, T.G., Cryan, J.F., 2018. Short-chain fatty acids: microbial metabolites that alleviate stress-induced brain-gut axis alterations. J Physiol 596 (20), 4923–4944.

van de Wouw, M., Lyte, J.M., Boehme, M., Sichetti, M., Moloney, G., Goodson, M.S., Kelley-Loughnane, N., Dinan, T.G., Clarke, G., Cryan, J.F., 2020a. The role of the

microbiota in acute stress-induced myeloid immune cell trafficking. Brain Behav Immun 84, 209–217.

van de Wouw, M., Sichetti, M., Long-Smith, C.M., Ritz, N.L., Moloney, G.M., Cusack, A. M., Berding, K., Dinan, T.G., Cryan, J.F., 2021. Acute stress increases monocyte levels and modulates receptor expression in healthy females. Brain Behav Immun 94, 463–468.

van de Wouw, M., Walsh, A.M., Crispie, F., van Leuven, L., Lyte, J.M., Boehme, M., Clarke, G., Dinan, T.G., Cotter, P.D., Cryan, J.F., 2020b. Distinct actions of the fermented beverage kefir on host behaviour, immunity and microbiome gut-brain modules in the mouse. Microbiome 8 (1), 67.

Vargas, D.L., Nascimbene, C., Krishnan, C., Zimmerman, A.W., Pardo, C.A., 2005. Neuroglial activation and neuroinflammation in the brain of patients with autism. Ann Neurol 57 (1), 67–81.

Vuong, H.E., Hsiao, E.Y., 2017. Emerging Roles for the Gut Microbiome in Autism Spectrum Disorder. Biol Psychiatry 81 (5), 411–423.

Walsh, A.M., Crispie, F., Kilcawley, K., O'Sullivan, O., O'Sullivan, M.G., Claesson, M.J., Cotter, P.D., 2016. Microbial Succession and Flavor Production in the Fermented Dairy Beverage Kefir. mSystems 1 (5), e00052–00016.

Weinstein-Fudim, L., Ergaz, Z., Turgeman, G., Yanai, J., Szyf, M., Ornoy, A., 2019. Gender Related Changes in Gene Expression Induced by Valproic Acid in A Mouse Model of Autism and the Correction by S-adenosyl Methionine. Does It Explain the Gender Differences in Autistic Like Behavior? Int J Mol Sci 20 (21).

Wickham, H., M. Averick, J. Bryan, W. Chang, L. D'Agostino McGowan, R. François, G. Grolemund, A. Hayes, L. Henry, J. Hester, M. Kuhn, T. L. Pedersen, E. Miller, A. M. Bache, K. Müller, J. Ooms, D. Robinson, D. P. Seidel, V. Spinu, K. Takahashi, D. Vaughan, C. Wilke, K. Woo and H. Yutani (2019). "Tidyverse.".

Wohleb, E.S., Powell, N.D., Godbout, J.P., Sheridan, J.F., 2013. Stress-induced recruitment of bone marrow-derived monocytes to the brain promotes anxiety-like behavior. J Neurosci 33 (34), 13820–13833.

Zhang, Q., Zou, R., Guo, M., Duan, M., Li, Q., Zheng, H., 2021. Comparison of gut microbiota between adults with autism spectrum disorder and obese adults. PeerJ 9, e10946.

Zhang, Y., Gao, D., Kluetzman, K., Mendoza, A., Bolivar, V.J., Reilly, A., Jolly, J.K., Lawrence, D.A., 2013. The maternal autoimmune environment affects the social behavior of offspring. J Neuroimmunol 258 (1–2), 51–60.

Zheng, H.-F., Wang, W.-Q., Li, X.-M., Rauw, G., Baker, G.B., 2017. Body fluid levels of neuroactive amino acids in autism spectrum disorders: a review of the literature. Amino Acids 49 (1), 57–65.

Zou, M., Li, D., Wang, L., Li, L., Xie, S., Liu, Y.u., Xia, W., Sun, C., Wu, L., 2020. Identification of Amino Acid Dysregulation as a Potential Biomarker for Autism Spectrum Disorder in China. Neurotox Res 38 (4), 992–1000.